

# Adaptive Video Streaming for Wireless Networks with Multiple Users and Helpers

D. Bethanabhotla, G. Caire and M. J. Neely

## Abstract

We consider the optimal design of a scheduling policy for adaptive video streaming in a wireless network formed by several users and helpers (e.g., base stations). A feature of such networks is that any user is typically in the range of multiple helpers. Hence, in order to cope with user-helper association, load balancing and inter-cell interference, an efficient streaming policy should allow the users to dynamically select the helper node to download from, and determine adaptively the video quality level of the download. In order to obtain a tractable formulation, we follow a “divide and conquer” approach: i) Assuming that each video packet (chunk) is delivered within its playback delay (“smooth streaming regime”), the problem is formulated as a network utility maximization (NUM), subject to queue stability, where the network utility function is a concave and componentwise non-decreasing function of the users’ video quality measure. ii) We solve the NUM problem by using a Lyapunov Drift Plus Penalty approach, obtaining a scheme that naturally decomposes into two sub-policies referred to as “congestion control” (adaptive video quality and helper station selection) and “transmission scheduling” (dynamic allocation of the helper-user physical layer transmission rates). Our solution is provably optimal with respect to the proposed NUM problem, in a strong per-sample path sense. iii) Finally, we propose a method to adaptively estimate the maximum queuing delays, such that each user can calculate its pre-buffering and re-buffering time in order to cope with the fluctuations of the queuing delays. In this way, the system can be forced to work in the smooth streaming regime, so that our NUM solution becomes fully relevant for the end user video quality. Through simulations, we evaluate the performance of the proposed algorithm under realistic assumptions of a network with densely deployed helper nodes, and demonstrate the per-sample path optimality of the proposed solution by considering a non-stationary non-ergodic scenario with user mobility, variable bit-rate video coding, and users joining or leaving the system at arbitrary times.

## Index Terms

Adaptive Video Streaming, Small-Cells Wireless Networks, Scheduling, Congestion Control, Adaptive Pre-Buffering Time.

The authors are with the Department of Electrical Engineering, University of Southern California, Los Angeles CA. Email: bethanab, caire, mjneely@usc.edu

## I. INTRODUCTION

Wireless data traffic is predicted to increase dramatically in the next few years, up to two orders of magnitude by 2020 [1]. This increase is mainly due to on-demand video streaming, enabled by multimedia devices such as tablets and smartphones. It is well understood that the current trend of cellular technology (e.g., LTE [2]) cannot cope with such traffic increase, unless the density of the deployed wireless infrastructure is increased correspondingly. This motivates the recent flurry of research on massive and dense deployment of base station antennas, either in the form of “massive MIMO” solutions (hundreds of antennas at each cell site [3]–[5]) or in the form of very dense small-cell networks (multiple nested tiers of smaller and smaller cells, possibly operating at higher and higher carrier frequencies [6]–[8]). While discussing the relative merits of these approaches is out of the scope of this paper, we mention here that the small-cell solution appears to be particularly attractive to handle a high density of nomadic (low mobility) users demanding high data rates, as for typical on-demand video streaming users.

Motivated by these considerations, in this paper we envisage a network formed by densely deployed fixed nodes (hereafter denoted as “helpers”), serving multiple stationary or low-mobility (nomadic) video-streaming users. We focus on on-demand video streaming, where users start their streaming sessions at random times, and demand different video files. Hence, the approach of having all users overhearing a common multicasting data stream, as in live streaming, is not applicable. In contrast, each streaming user requests sequentially a number of video segments (referred to as chunks) and starts its playback after a delay much smaller than the duration of the its streaming session. In order to guarantee “smooth streaming”, the system has to ensure that each video segment is delivered before its playback deadline. This fundamentally differentiates the streaming problem from the file downloading problem.

This paper focuses on the problem of joint transmission scheduling and congestion control for adaptive video streaming in a wireless network formed by many users and helpers deployed over a localized geographic area and sharing the same channel bandwidth. We focus on the wireless segment of the network, assuming that the video files are already present at the helper nodes. This condition holds when the backhaul connecting the helper nodes to some video server (or a content distribution network) in the core network is fast enough such that we can neglect the delays introduced by the backhaul. In the case where such fast backhaul is not present, we have recently proposed and studied a novel approach nicknamed *FemtoCaching*, where the inherent *asynchronous content reuse* of on-demand video streaming is exploited in order to predict and proactively store the popular video files such that, with high probability, the demanded files are effectively already present in the helpers’ caches [9]–[14]. The trend of caching

at the wireless edge has raised significant interest (see also [15]–[20]), and justifies our assumption of neglecting the effects of the wired backhaul and focus only on the wireless segment of the system.

**Contributions:** In order to obtain a tractable formulation, we follow a “divide and conquer” approach. First, we assume that under queue stability all requested bits are delivered within some finite bounded delay such that, if a user playback buffer is larger than the largest queuing delay experienced by that user, then all video chunks will be delivered within their playback deadline. We refer to the regime where this happens with high probability as the “smooth streaming regime”. Under the smooth streaming regime assumption, we formulate the system optimality directly in terms of the users’ video qualities subject to the stability of all queues in the system. This yields a Network Utility Maximization (NUM) problem [21]–[23], that we solve in the framework of Lyapunov Optimization [24], using the *drift plus penalty* (DPP) approach [24]. The obtained solution is provably asymptotically optimal (with respect to the defined NUM problem) on a per-sample path sense (i.e., without assuming stationarity and ergodicity of the underlying network state process [24], [25]). Furthermore, it naturally decomposes into sub-policies that can be implemented in a layered and distributed way, by functions performed at the users and the helpers, requiring only “local” information. The sub-policy implemented at the user nodes is referred to as “congestion control”, since it consists of the adaptive selection of the video quality and the serving helper. The sub-policy implemented at the helpers is referred to as “transmission scheduling”, since it corresponds to the adaptive selection of the user to be served on the downlink of each helper station. Then, we deal with the fact that, in reality, the system is not automatically guaranteed to work in the smooth streaming regime. Hence, we have to explicitly take into account the fact that some video packets may not meet their playback deadline. In order to cope with this problem, we propose a method to locally estimate the delays with which the video packets are delivered, such that each user can calculate its pre-buffering and re-buffering time in order to make the probability of “stall events” during the streaming session very small. In particular, when the maximum delay of each queue in the system admits a deterministic upper bound, the proposed scheme eliminates stall events completely. Through simulations, we evaluate the performance of the proposed scheduling policy and adaptive pre-buffering algorithm under realistic assumptions for a small-cell network and demonstrate the per-sample path optimality of the proposed solution by considering a non-stationary non-ergodic scenario with user mobility, variable bit-rate (VBR) video coding [26], and users joining or leaving the system at arbitrary times. It follows that if the size of the playback buffers is appropriately dimensioned using our proposed adaptive scheme, the system effectively works in the smooth streaming regime, and the maximization of the proposed network utility function subject to queue stability yields effectively near-optimal performance, for any network configuration, and

without assumption on stationarity and ergodicity of the video data rate per chunk and/or of the channel pathloss coefficients (which are slowly arbitrarily varying according to the users' motion).

The rest of this paper is organized as follows. In Section II, we describe the system model for on-demand video streaming in a wireless network with many users and helpers, and discuss some key underlying assumptions. In Section III, we formulate the NUM problem, provide the proposed distributed dynamic scheduling policy for its solution, and state the main results on its optimality. Section IV illustrates our proposed scheme for adaptive pre-buffering and re-buffering in order to cope with stall events. Finally, simulation results illustrating the particular features of the proposed scheme are provided in Section V. The main technical proofs are collected in the Appendices, in order to maintain the flow of exposition.

## II. SYSTEM MODEL

We consider a discrete, time-slotted wireless network with multiple users and multiple helper stations sharing the same bandwidth. The network is defined by a bipartite graph  $\mathcal{G} = (\mathcal{U}, \mathcal{H}, \mathcal{E})$ , where  $\mathcal{U}$  denotes the set of users,  $\mathcal{H}$  denotes the set of helpers, and  $\mathcal{E}$  contains edges for all pairs  $(h, u)$  such that there exists a potential transmission link between  $h \in \mathcal{H}$  and  $u \in \mathcal{U}$ .<sup>1</sup> We denote by  $\mathcal{N}(u) \subseteq \mathcal{H}$  the neighborhood of user  $u$ , i.e.,  $\mathcal{N}(u) = \{h \in \mathcal{H} : (h, u) \in \mathcal{E}\}$ . Similarly,  $\mathcal{N}(h) = \{u \in \mathcal{U} : (h, u) \in \mathcal{E}\}$ .

Each user  $u \in \mathcal{U}$  requests a video file  $f_u$  from a library  $\mathcal{F}$  of possible files. Each video file is formed by a sequence of chunks. Each chunk corresponds to a group of pictures (GOP) that are encoded and decoded as stand-alone units [27]. Chunks have a fixed playback duration, given by  $T_{\text{gop}} = (\# \text{ frames per GOP})/\eta$ , where  $\eta$  is the frame rate, expressed in frames per second. The streaming process consists of transferring chunks from the helpers to the requesting users such that the playback buffer at each user contains the required chunks at the beginning of each chunk playback deadline. The playback starts after a short pre-buffering time, during which the playback buffer is filled by a determined amount of ordered chunks. The details relative to pre-buffering and chunk playback deadlines are discussed in Section IV.

The helpers may not have access to the whole video library, because of backhaul constraints or caching constraints.<sup>2</sup> In general, we denote by  $\mathcal{H}(f)$  the set of helpers that contain file  $f \in \mathcal{F}$ . Hence, user  $u$  requesting file  $f_u$  can only download video chunks from helpers in the set  $\mathcal{N}(u) \cap \mathcal{H}(f_u)$ .

<sup>1</sup>The existence of such potential links depends on the channel gain coefficients between helper  $h$  and user  $u$  (see the physical channel model in Section II-A), as well as on some protocol imposing restricted access for some helpers.

<sup>2</sup>For example, in a FemtoCaching network (see discussion in Section I) each helper contains a subset of the files depending on some caching algorithm.

Each file  $f \in \mathcal{F}$  is encoded at a finite number of different quality levels  $m \in \{1, \dots, N_f\}$ . This is similar to the implementation of several current video streaming technologies, such as Microsoft Smooth Streaming and Apple HTTP Live Streaming [28]. Due to the VBR nature of video coding [26], the quality-rate profile of a given file  $f$  may vary from chunk to chunk. We let  $D_f(m, t)$  and  $B_f(m, t)$  denote the video quality measure (e.g., see [29]) and the number of bits per pixel for file  $f$  at chunk time  $t$  and quality level  $m$  respectively.

A scheduling policy for the network at hand consists of a sequence of decisions such that, at each chunk time  $t$ , each streaming user  $u$  requests its desired  $t$ -th chunk of file  $f_u$  from one or more helpers in  $\mathcal{N}(u) \cap \mathcal{H}(f_u)$  at some quality level  $m$ , and each helper  $h$  transmits the source-encoded bits of currently or previously requested chunks to the users. We assume that the scheduler time-scale coincides with the chunk interval, i.e., at each chunk interval a scheduling decision is made. Conventionally, we assume a slotted time axis  $t = 0, 1, 2, 3, \dots$ , corresponding to epochs  $t \times T_{\text{gop}}$ . Letting  $T_u$  denote the pre-buffering delay of user  $u$  (where  $T_u$  is an integer number of chunk times), the chunks are downloaded starting at time  $t = 0$  and the  $t$ -th chunk playback deadline is  $t + T_u$ . A stall event for user  $u$  is defined as the event that the playback buffer does not contain chunk number  $t - T_u$  at slot time  $t$ .

Letting  $N_{\text{pix}}$  denote the number of pixels per frame, a chunk contains  $k = \eta T_{\text{gop}} N_{\text{pix}}$  pixels. Hence, the number of bits in the  $t$ -th chunk of file  $f$ , encoded at quality level  $m$ , is given by  $kB_f(m, t)$ . We assume that a chunk can be partially downloaded from multiple helpers, and let  $R_{hu}(t)$  denote the source coding rate (bit per pixel) of chunk  $t$  requested by user  $u$  from helper  $h$ . It follows that the source coding rates must satisfy, for all  $t$ ,

$$\sum_{h \in \mathcal{N}(u) \cap \mathcal{H}(f_u)} R_{hu}(t) = B_{f_u}(m_u(t), t), \quad \forall (h, u) \in \mathcal{E}, \quad (1)$$

where  $m_u(t)$  denotes the quality level at which chunk  $t$  of file  $f_u$  is requested by user  $u$ . The constraint (1) reflects the fact that the aggregate bits of a given chunk  $t$  from all helpers serving user  $u$  must be equal to the total number of bits in the requested chunk. When a chunk request is made and the source coding rates  $R_{hu}(t)$  are determined, helper  $h$  places the corresponding  $kR_{hu}(t)$  bits in a transmission queue  $Q_{hu}$  “pointing” at user  $u$ . This queue contains the source-encoded bits that have to be sent from helper  $h$  to user  $u$ . Notice that in order to be able to download different parts of the same chunk from different helpers, the network controller needs to ensure that all received bits from the serving helpers  $\mathcal{N}(u) \cap \mathcal{H}(f_u)$  are useful, i.e., the union of all requested bits yields the total bits in the requested chunk, without overlaps or gaps. Alternatively, each chunk can be encoded by intra-session *Random Linear Network Coding* [30] such that as long as  $kB_{f_u}(m_u(t), t)$  parity bits are collected at user  $u$ , the  $t$ -th

chunk can be decoded and it becomes available in the user playback buffer. Interestingly, even though we optimize over algorithms that allow the possibility of downloading different bits of the same chunk from different helpers, the optimal scheduling policy (derived in Section III) has a simple structure that always requests entire chunks from single helpers. Hence, without loss of optimality, neither protocol coordination to prevent overlaps or gaps, nor intra-session linear network coding, are needed for the algorithm implementation.

#### A. Wireless transmission channel

We model the wireless channel for each link  $(h, u) \in \mathcal{E}$  as a frequency and time selective underspread fading channel [31]. Using OFDM, the channel can be converted into a set of parallel narrowband subchannels in the frequency domain (subcarriers), each of which is time-selective with a certain fading channel coherence time. The small-scale Rayleigh fading channel coefficients can be considered as constant over time-frequency “tiles” spanning blocks of adjacent subcarriers in the frequency domain and blocks of OFDM symbols in the time domain. For example, in the LTE standard [2], the small scale fading coefficients can be considered constant over a coherence time interval of 0.5 ms and a coherence bandwidth of 180 kHz, corresponding to “tiles” of 7 OFDM symbols  $\times$  12 subcarriers. For a total system available bandwidth of 18MHz (after excluding the guard bands) and a scheduling slot of duration  $T_{\text{gop}} = 0.5\text{s}$  (typical video chunk duration), we have that a scheduling slot spans  $\frac{0.5 \times 18 \cdot 10^6}{0.5 \cdot 10^{-3} \times 180 \cdot 10^3} = 10^5$  tiles, i.e., channel fading coefficients. Even assuming some correlation between fading coefficients, it is apparent that the time-frequency diversity experienced in the transmission of a chunk is *very large*. Thus, it is safe to assume that channel coding over such a large number of resource blocks achieves the *ergodic capacity* of the underlying fading channel.

In this paper we refer to *ergodic capacity* as the *average* mutual information resulting from Gaussian i.i.d. inputs of the single-user channel from helper  $h$  and user  $u \in \mathcal{N}(h)$ , while treating the inter-cell interference, i.e., the signals of all other helpers  $h' \neq h$  as noise, where averaging is with respect to the first-order distribution of the small-scale fading. This rate is achievable by i.i.d. Gaussian coding ensembles and approachable in practice by modern graph-based codes [32] provided that the length of a codeword spans a large number of independent small-scale fading states [33].

We assume that the helpers transmit at constant power, and that the small-cell network makes use of universal frequency reuse, that is, the whole system bandwidth is used by all the helper stations. We further assume that every user  $u$ , when decoding a transmission from a particular helper  $h \in \mathcal{N}(u)$  treats

inter-cell interference as noise. Under these system assumptions, the maximum achievable rate<sup>3</sup> at slot time  $t$  for link  $(h, u) \in \mathcal{E}$  is given by

$$C_{hu}(t) = \mathbb{E} \left[ \log \left( 1 + \frac{P_h g_{hu}(t) |s_{hu}|^2}{1 + \sum_{\substack{h' \neq h \\ h' \in \mathcal{N}(u)}} P_{h'} g_{h'u}(t) |s_{h'u}|^2} \right) \right], \quad (2)$$

where  $P_h$  is the transmit power of helper  $h$ ,  $s_{hu}$  is the small-scale fading gain from helper  $h$  to user  $u$  and  $g_{hu}(t)$  is the slow fading gain (path loss) from helper  $h$  to user  $u$ . Notice that at the denominator of the Signal to Interference plus Noise Ratio (SINR) inside the logarithm in (2) we have the sum of the signal powers of all helpers  $h' \in \mathcal{N}(u) : h' \neq h$ , indicating the inter-cell interference suffered from user  $u$ , when decoding the transmission from helper  $h$ .

In this work, consistently with most current wireless standards, we consider the case of intra-cell orthogonal access. This means that each helper  $h$  serves its neighboring users  $u \in \mathcal{N}(h)$  using orthogonal FDMA/TDMA. It follows that the feasible set of channel coding rates  $\{\mu_{hu}(t) : u \in \mathcal{N}(h)\}$  for each helper  $h$  must satisfy the constraint:

$$\sum_{u \in \mathcal{N}(h)} \frac{\mu_{hu}(t)}{C_{hu}(t)} \leq 1, \quad \forall h \in \mathcal{H}. \quad (3)$$

The underlying assumption, which makes the rate region defined in (3) achievable, is that helper  $h$  is aware of the slowly varying path loss coefficients  $g_{hu}(t)$  for all  $u \in \mathcal{N}(h)$ , such that rate adaptation is possible. This is consistent with currently implemented rate adaptation schemes [2], [34], [35].

## B. Transmission queues dynamics and network state

The dynamics (time evolution) of the transmission queues at the helpers is given by:

$$Q_{hu}(t+1) = \max\{Q_{hu}(t) - n\mu_{hu}(t), 0\} + kR_{hu}(t), \quad \forall (h, u) \in \mathcal{E}, \quad (4)$$

where  $n$  denotes the number of physical layer channel symbols corresponding to the duration  $T_{\text{gop}}$ , and  $\mu_{hu}(t)$  is the channel coding rate (bits/channel symbol) of the transmission from helper  $h$  to user  $u$  at time  $t$ . Notice that (4) reflects the fact that at any chunk time  $t$  the requested amount  $kR_{hu}(t)$  of source-encoded bits is input to the queue of helper  $h$  serving user  $u$ , and up to  $n\mu_{hu}(t)$  source-encoded bits are extracted from the same queue and delivered by helper  $h$  to user  $u$  over the wireless channel.

<sup>3</sup> We express channel coding rates  $\mu_{hu}$  in bit/s/Hz, i.e., bit per complex channel symbol use and the source coding rates  $R_{hu}$  in bit/pixel, i.e., bits per source symbol, in agreement with standard information theoretic channel coding and source coding.

The channel coefficients  $g_{hu}(t)$  models path loss and shadowing between helper  $h$  and user  $u$ , and are assumed to change slowly in time. For a typical small-cell scenario with nomadic users moving at walking speed or slower, the path loss coefficients change on a time-scale of the order of 10s (i.e.,  $\approx 20$  scheduling slots). This time scale is much slower than the coherence of the small-scale fading, but it is comparable with the duration of the video chunks. Therefore, variations of these coefficients during a streaming session (e.g., due to user mobility) are relevant. At this point, we can formally define the network state and a feasible scheduling policy for our system.

*Definition 1:* The network state  $\omega(t)$  collects the quantities that evolve independently of the scheduling decisions in the network. These are, in particular, the slowly-varying channel gains, the video quality levels, and the corresponding bit-rates of the chunk at time  $t$ . Hence, we have

$$\omega(t) = \{g_{hu}(t), D_{f_u}(\cdot, t), B_{f_u}(\cdot, t) : \forall (h, u) \in \mathcal{E}\}. \quad (5)$$

◇

*Definition 2:* A scheduling policy  $\{a(t)\}_{t=0}^{\infty}$  is a sequence of control actions  $a(t)$  comprising the vector  $\mathbf{R}(t)$  with elements  $kR_{hu}(t)$  of requested source-coded bits, the vector  $\boldsymbol{\mu}(t)$  with elements  $n\mu_{hu}(t)$  of transmitted channel-coded bits, and the quality level decisions  $\{m_u(t) : \forall u \in \mathcal{U}\}$ . ◇

*Definition 3:* For any  $t$ , the feasible set of control actions  $A_{\omega(t)}$  includes all control actions  $a(t)$  such that the constraints (1) and (3) are satisfied. ◇

*Definition 4:* A feasible scheduling policy for the system at hand is a sequence of control actions  $\{a(t)\}_{t=0}^{\infty}$  such that  $a(t) \in A_{\omega(t)}$  for all  $t$ . ◇

### III. PROBLEM FORMULATION AND OPTIMAL SCHEDULING POLICY

The goal of a scheduling policy for our system is to maximize a concave *network utility function* of the individual users' video qualities. Since these are time-varying quantities, we focus on the time average of such qualities. In addition, all source-coded bits requested by the users should be delivered. This imposes the constraint that all transmission queues at the helpers must be stable. Throughout this work, we use the following standard notation for the time average expectation of any quantity  $x$ :

$$\bar{x} := \lim_{t \rightarrow \infty} \frac{1}{t} \sum_{\tau=0}^{t-1} \mathbb{E}[x(\tau)]. \quad (6)$$

We define  $\bar{D}_u := \lim_{t \rightarrow \infty} \frac{1}{t} \sum_{\tau=0}^{t-1} \mathbb{E}[D_{f_u}(m_u(\tau), \tau)]$  to be the time average of the expected quality of user  $u$ , and  $\bar{Q}_{hu} := \lim_{t \rightarrow \infty} \frac{1}{t} \sum_{\tau=0}^{t-1} \mathbb{E}[Q_{hu}(\tau)]$  to be the time average of the expected length of the

queue at helper  $h$  for data transmission to user  $u$ , assuming temporarily that these limits exist.<sup>4</sup> Let  $\phi_u(\cdot)$  be a concave, continuous, and non-decreasing function defining network utility vs. video quality for user  $u \in \mathcal{U}$ . Then, the proposed scheduling policy is the solution of the following NUM problem:

$$\begin{aligned} & \text{maximize} && \sum_{u \in \mathcal{U}} \phi_u(\bar{D}_u) \\ & \text{subject to} && \bar{Q}_{hu} < \infty \quad \forall (h, u) \in \mathcal{E} \\ & && a(t) \in A_{\omega(t)} \quad \forall t, \end{aligned} \tag{7}$$

where requirement of finite  $\bar{Q}_{hu}$  corresponds to the *strong stability* condition for all the queues [24].

By appropriately choosing the functions  $\phi_u(\cdot)$ , we can impose some desired notion of fairness. For example, a general class of concave functions suitable for this purpose is given by the  $\alpha$ -fairness network utility, defined by [36]

$$\phi_u(x) = \begin{cases} \log x & \alpha = 1 \\ \frac{x^{1-\alpha}}{1-\alpha} & \alpha > 0, \quad \alpha \neq 1 \end{cases} \tag{8}$$

In this case, it is well-known that  $\alpha = 0$  yields the maximization of the sum quality (no fairness),  $\alpha \rightarrow \infty$  yields the maximization of the worst-case quality (max-min fairness) and  $\alpha = 1$  yields the maximization of the geometric mean quality (proportional fairness).

**Remark 1:** *On the relevance of NUM problem (7) for video streaming.* A natural objection to our problem formulation is that queue stability does not necessarily guarantee that the chunks are delivered by their playback deadline, but only that the chunks “will be eventually delivered”. As explained in Section I, in order to obtain a clean and tractable problem leading to a low complexity and low-overhead decentralized protocol, we have assumed that all users work in the regime of smooth streaming. In particular, for any given  $u \in \mathcal{U}$ , if the playback buffer is larger than the maximum delay introduced by queues  $Q_{hu}(t)$ , for all  $h \in \mathcal{N}(u)$ , then the streaming process of user  $u$  finds all chunks in the buffer before their corresponding playback deadline (zero stall probability). In this condition, the NUM problem (7) is effectively relevant to maximize the user video qualities with respect to the desired fairness criterion. In Section IV we propose a scheme to adaptively dimension the playback buffer of each user based on the measured maximum queuing delay in a sliding window. Such scheme makes the system work in the regime of small stall probability (the smooth streaming regime). This justifies the constrained maximization in (7) as effectively relevant for the actual users’ video quality.  $\diamond$

<sup>4</sup>The existence of these limits is assumed temporarily for ease of exposition of the optimization problem (7) but is not required for the derivation of the scheduling policy and for the proof of Theorem 1.

In the following, we first illustrate a dynamic scheduling policy for problem (7). Then, Theorem 1 states the optimality guarantee of the proposed dynamic scheduling policy in a strong per-sample path sense, in the sense of approaching, within any desired accuracy, the maximum of the NUM problem (7) over all (genie-aided) policies with look-ahead over a given sample path.

#### A. Dynamic scheduling policy

We introduce auxiliary variables  $\gamma_u(t)$  and corresponding virtual queues  $\Theta_u(t)$  with buffer evolution:

$$\Theta_u(t+1) = \max \{ \Theta_u(t) + \gamma_u(t) - D_{f_u}(m_u(t), t), 0 \}. \quad (9)$$

Each user  $u \in \mathcal{U}$  updates its own virtual queue  $\Theta_u(t)$  locally. Also, we introduce a scheduling policy control parameter  $V > 0$  that trades off the average queue lengths with the accuracy with which the policy is able to approach the optimum of the NUM problem (7).

According to Definition 2, a scheduling policy is defined by specifying how to calculate the source-coding rates  $R_{hu}(t)$ , the video quality levels  $m_u(t)$ , and the channel coding rates  $\mu_{hu}(t)$ , for all chunk times  $t$ . These are given by solving local maximizations at each user node  $u$  and helper node  $h$ . Since these maximizations depend only on local variables that can be learned by each node from its neighbors through simple protocol signaling at negligible overhead cost (a few scalar quantities per chunk time), the resulting policy is decentralized.

1) *Control actions at the user nodes (congestion control)*: At time  $t$ , each  $u \in \mathcal{U}$  chooses the helper in its neighborhood having the desired file  $f_u$  and with the shortest queue, i.e.,

$$h_u^*(t) = \operatorname{argmin} \{ Q_{hu}(t) : h \in \mathcal{N}(u) \cap \mathcal{H}(f_u) \}. \quad (10)$$

Then, it determines the quality level  $m_u(t)$  of the requested chunk at time  $t$  as:

$$m_u(t) = \operatorname{argmin} \{ kQ_{h_u^*(t)u}(t)B_{f_u}(m, t) - \Theta_u(t)D_{f_u}(m, t) : m \in \{1, \dots, N_{f_u}\} \}. \quad (11)$$

The source coding rates for the requested chunk at time  $t$  are given by:

$$R_{hu}(t) = \begin{cases} B_{f_u}(m_u(t), t) & \text{for } h = h_u^*(t) \\ 0 & \text{for } h \neq h_u^*(t) \end{cases} \quad (12)$$

The virtual queue  $\Theta_u(t)$  is updated according to (9), where  $\gamma_u(t)$  is given by:

$$\gamma_u(t) = \operatorname{argmax} \{ V\phi_u(\gamma) - \Theta_u(t)\gamma : \gamma \in [D_u^{\min}, D_u^{\max}] \}, \quad (13)$$

where  $D_u^{\min}$  and  $D_u^{\max}$  are uniform lower and upper bounds on the quality function  $D_{f_u}(\cdot, t)$ .

We refer to the policy (10) – (13) as *congestion control* since each user  $u$  selects the helper from which to request the current video chunk and the quality at which this chunk is requested by taking into account the state of the transmission queues of all helpers  $h$  that potentially can deliver such chunk, and choosing the least congested queue (selection in (10)) and an appropriate video quality level that balances the desire for high quality (reflected by the term  $-\Theta_u(t)D_{f_u}(m, t)$  in (11)) and the desire for low transmission queues (reflected by the term  $kQ_{h_u^*(t)u}(t)B_{f_u}(m, t)$  in (11)). Notice that the streaming of the video file  $f_u$  may be handled by *different* helpers across the streaming session, but each individual chunk is entirely downloaded from a single helper. Notice also that in order to compute (10) – (13) each user needs to know only *local information* formed by the queue backlogs  $Q_{hu}(t)$  of its neighboring helpers, and by the locally computed virtual queue backlog  $\Theta_u(t)$ .

The above congestion control action at the users is reminiscent of the current adaptive streaming technology for video on demand systems, referred to as DASH (Dynamic Adaptive Streaming over HTTP) [27], [37], where the client (user) progressively fetches a video file by downloading successive chunks, and makes adaptive decisions on the quality level based on its current knowledge of the congestion of the underlying server-client connection. Our policy generalizes DASH by allowing the client  $u$  to dynamically select the least backlogged server  $h_u^*(t)$ , at each chunk time  $t$ .

2) *Control actions at the helper nodes (transmission scheduling)*: At time  $t$ , the general transmission scheduling consists of maximizing the weighted sum rate of the transmission rates achievable at scheduling slot  $t$ . Namely, the network of helpers must solve the Max-Weighted Sum Rate (MWSR) problem:

$$\begin{aligned} & \text{maximize} && \sum_{h \in \mathcal{H}} \sum_{u \in \mathcal{N}(h)} Q_{hu}(t) \mu_{hu}(t) \\ & \text{subject to} && \boldsymbol{\mu}(t) \in \mathcal{R}(t) \end{aligned} \tag{14}$$

where  $\mathcal{R}(t)$  is the region of achievable rates supported by the network at time  $t$ . In this work, we consider two different physical layer assumptions, yielding to two versions of the above general MWSR problem.

In the first case, referred to as “macro-diversity”, the users can decode multiple data streams from multiple helpers if they are scheduled with non-zero rate on the same slot. Notice that, consistently with (2) and (3), this does not contradict the fact that interference is treated as noise and that each helper uses orthogonal intra-cell access.<sup>5</sup> In the macro-diversity case, the rate region  $\mathcal{R}(t)$  is given by the Cartesian

<sup>5</sup>As a matter of fact, if a user is scheduled with non-zero rate at more than one helper, it could use successive interference cancellation or joint decoding of all its intended data streams. Nevertheless, we assume here, conservatively, that interference (even from the intended streams) is treated as noise.

product of the orthogonal access regions (3), such that the general MWSR problem (14) decomposes into individual problems, to be solved in a decentralized way at each helper node. After the change of variables  $\nu_{hu}(t) = \frac{\mu_{hu}(t)}{C_{hu}(t)}$ , it is immediate to see that (14) reduces to the set of decoupled *Linear Programs* (LPs):

$$\begin{aligned} & \text{maximize} && \sum_{u \in \mathcal{N}(h)} Q_{hu}(t) C_{hu}(t) \nu_{hu}(t) \\ & \text{subject to} && \sum_{u \in \mathcal{N}(h)} \nu_{hu}(t) \leq 1, \end{aligned} \quad (15)$$

for all  $h \in \mathcal{H}$ . The feasible region of (15) is the  $|\mathcal{N}(h)|$ -dimensional simplex and the solution is given by the vertex corresponding to user  $u_h^*(t)$  given by

$$u_h^*(t) = \operatorname{argmax} \{Q_{hu}(t) C_{hu}(t) : u \in \mathcal{N}(h)\}, \quad (16)$$

with rate vector given by  $\mu_{hu_h^*(t)}(t) = C_{hu_h^*(t)}(t)$  and  $\mu_{hu}(t) = 0$  for all  $u \neq u_h^*(t)$ .

In the second case, referred to as “unique association”, any user can receive data from not more than a single helper on any scheduling slot. In this case, the MWSR problem reduces to a maximum weighted matching problem that can be solved by an LP as follows. We introduce variables  $\alpha_{hu}(t)$  such that  $\alpha_{hu}(t) = 1$  if user  $u$  is served by helper  $h$  at time  $t$  and  $\alpha_{hu}(t) = 0$  if it is not. It is obvious that if  $\alpha_{hu}(t) = 1$ , then  $\mu_{hu}(t) = C_{hu}(t)$ , implying that  $\mu_{h'u}(t) = 0$  for all  $h' \neq h$  and  $\mu_{hu'}(t) = 0$  for all  $u' \neq u$  (by (3)). Hence, (14) in this case reduces to

$$\begin{aligned} & \text{maximize} && \sum_{h \in \mathcal{H}} \sum_{u \in \mathcal{N}(h)} \alpha_{hu}(t) Q_{hu}(t) C_{hu}(t) \\ & \text{subject to} && \sum_{h \in \mathcal{N}(u)} \alpha_{hu}(t) \leq 1 \quad \forall u \in \mathcal{U}, \\ & && \sum_{u \in \mathcal{N}(h)} \alpha_{hu}(t) = 1 \quad \forall h \in \mathcal{H}, \\ & && \alpha_{hu}(t) \in \{0, 1\}, \quad \forall h \in \mathcal{H}, u \in \mathcal{U}. \end{aligned} \quad (17)$$

A well-known result (see [38, Theorem 64.7]) states that, since the network graph  $\mathcal{G} = (\mathcal{U}, \mathcal{H}, \mathcal{E})$  is bipartite, the integer programming problem (17) can be relaxed to an LP by replacing the integer constraints on  $\{\alpha_{hu}(t)\}$  with the linear constraints  $\alpha_{hu}(t) \in [0, 1]$  for all  $h \in \mathcal{H}$ ,  $u \in \mathcal{U}$ . The solution of the relaxed LP is guaranteed to be integral, such that it is feasible (and therefore optimal) for (17). Notice that, in the case of unique association, the rate scheduling problem does not admit a decoupled solution, calculated independently at each helper node. Hence, a network controller that solves (17) and

allocates the downlink rates (and the user-helper dynamic association) at each slot time  $t$  is required. Again, since  $t$  ticks at the chunk time, i.e., on the time scale of seconds, this does not involve a very large complexity, although it is definitely more complex than the macro-diversity case.

**Remark 2:** *Dynamic helper-user association.* Notice that here, unlike conventional cellular systems, we do not assign a fixed set of users to each helper. In contrast, the helper-user association is dynamic, and results from the transmission scheduling decision. Notice also that, for both the macro-diversity and the unique association cases, despite the fact that each helper  $h$  is allowed to serve its queues with rates  $\mu_{hu}(t)$  satisfying (3), the proposed policy allocates the whole  $t$ -th downlink slot to a single user  $u \in \mathcal{N}(h)$ , served at its own peak-rate  $C_{hu}(t)$ . This is reminiscent of opportunistic user selection in high-rate downlink schemes of 3G cellular systems, such as HSDPA and Ev-Do [2], [39].  $\diamond$

### B. Derivation of the scheduling policy

In order to solve problem (7) using the stochastic optimization theory developed in [24], it is convenient to transform it into an equivalent problem that involves the maximization of a single time average. This transformation is achieved through the use of auxiliary variables  $\gamma_u(t)$  and the corresponding virtual queues  $\Theta_u(t)$  with buffer evolution given in (9). Consider the transformed problem:

$$\text{maximize } \sum_{u \in \mathcal{U}} \overline{\phi_u(\gamma_u)} \quad (18)$$

$$\text{subject to } \overline{Q}_{hu} < \infty \quad \forall (h, u) \in \mathcal{E} \quad (19)$$

$$\overline{\gamma}_u \leq \overline{D}_u \quad \forall u \in \mathcal{U} \quad (20)$$

$$D_u^{\min} \leq \gamma_u(t) \leq D_u^{\max} \quad \forall u \in \mathcal{U} \quad (21)$$

$$a(t) \in A_{\omega(t)} \quad \forall t \quad (22)$$

Notice that constraints (20) correspond to stability of the virtual queues  $\Theta_u$ , since  $\overline{\gamma}_u$  and  $\overline{D}_u$  are the time-averaged arrival rate and the time-averaged service rate for the virtual queue given in (9). We have:

*Lemma 1:* Problems (7) and (18) – (22) are equivalent.  $\square$

*Proof:* See Appendix A.  $\blacksquare$

Thanks to Lemma 1, we shall now focus on the solution of problem (18) – (22). Let  $\mathbf{Q}(t)$  denote the column vector containing the backlogs of queues  $Q_{hu} \quad \forall (h, u) \in \mathcal{E}$ , let  $\Theta(t)$  denote the column vector for the virtual queues  $\Theta_u \quad \forall u \in \mathcal{U}$ ,  $\gamma(t)$  denote the column vector with elements  $\gamma_u(t) \quad \forall u \in \mathcal{U}$ , and  $\mathbf{D}(t)$  denote the column vector with elements  $D_{f_u}(m_u(t), t) \quad \forall u \in \mathcal{U}$ . Let  $\mathbf{G}(t) = [\mathbf{Q}^T(t), \Theta^T(t)]^T$  be the

composite vector of queue backlogs and define the quadratic Lyapunov function  $L(\mathbf{G}(t)) = \frac{1}{2}\mathbf{G}^\top(t)\mathbf{G}(t)$ . The one-slot drift of the Lyapunov function at slot  $t$  is given by

$$\begin{aligned}
L(\mathbf{G}(t+1)) - L(\mathbf{G}(t)) &= \frac{1}{2} \left( \mathbf{Q}^\top(t+1)\mathbf{Q}(t+1) - \mathbf{Q}^\top(t)\mathbf{Q}(t) \right) + \frac{1}{2} \left( \boldsymbol{\Theta}^\top(t+1)\boldsymbol{\Theta}(t+1) - \boldsymbol{\Theta}^\top(t)\boldsymbol{\Theta}(t) \right) \\
&= \frac{1}{2} \left[ (\max\{\mathbf{Q}(t) - \boldsymbol{\mu}(t), \mathbf{0}\} + \mathbf{R}(t))^\top (\max\{\mathbf{Q}(t) - \boldsymbol{\mu}(t), \mathbf{0}\} + \mathbf{R}(t)) - \mathbf{Q}^\top(t)\mathbf{Q}(t) \right] \\
&\quad + \frac{1}{2} \left[ (\max\{\boldsymbol{\Theta}(t) + \boldsymbol{\gamma}(t) - \mathbf{D}(t), \mathbf{0}\})^\top (\max\{\boldsymbol{\Theta}(t) + \boldsymbol{\gamma}(t) - \mathbf{D}(t), \mathbf{0}\}) - \boldsymbol{\Theta}^\top(t)\boldsymbol{\Theta}(t) \right],
\end{aligned} \tag{23}$$

where we have used the queue evolution equations (4) and (9) and “max” is applied componentwise.

Noticing that for any non-negative scalar quantities  $Q, \mu, R, \Theta, \gamma$  and  $D$  we have the inequalities

$$(\max\{Q - \mu, 0\} + R)^2 \leq Q^2 + \mu^2 + R^2 + 2Q(R - \mu), \tag{24}$$

and

$$(\max\{\Theta + \gamma - D, 0\})^2 \leq (\Theta + \gamma - D)^2 = \Theta^2 + (\gamma - D)^2 + 2\Theta(\gamma - D), \tag{25}$$

we have

$$\begin{aligned}
L(\mathbf{G}(t+1)) - L(\mathbf{G}(t)) &\leq \frac{1}{2}\boldsymbol{\mu}^\top(t)\boldsymbol{\mu}(t) + \mathbf{R}^\top(t)\mathbf{R}(t) + (\mathbf{R}(t) - \boldsymbol{\mu}(t))^\top \mathbf{Q}(t) \\
&\quad + \frac{1}{2}(\boldsymbol{\gamma}(t) - \mathbf{D}(t))^\top (\boldsymbol{\gamma}(t) - \mathbf{D}(t)) + (\boldsymbol{\gamma}(t) - \mathbf{D}(t))^\top \boldsymbol{\Theta}(t)
\end{aligned} \tag{26}$$

$$\leq \mathcal{K} + (\mathbf{R}(t) - \boldsymbol{\mu}(t))^\top \mathbf{Q}(t) + (\boldsymbol{\gamma}(t) - \mathbf{D}(t))^\top \boldsymbol{\Theta}(t), \tag{27}$$

where  $\mathcal{K}$  is a uniform bound on the term  $\frac{1}{2}[\boldsymbol{\mu}^\top(t)\boldsymbol{\mu}(t) + \mathbf{R}^\top(t)\mathbf{R}(t)] + \frac{1}{2}(\boldsymbol{\gamma}(t) - \mathbf{D}(t))^\top (\boldsymbol{\gamma}(t) - \mathbf{D}(t))$ , which exists under the realistic assumption that the source coding rates, the channel coding rates and the video quality measures are upper bounded by some constants, independent of  $t$ . The conditional expected Lyapunov drift for slot  $t$  is defined by

$$\Delta(\mathbf{G}(t)) = \mathbb{E}[L(\mathbf{G}(t+1))|\mathbf{G}(t)] - L(\mathbf{G}(t)). \tag{28}$$

Adding on both sides the penalty term  $-V \sum_{u \in \mathcal{U}} \mathbb{E}[\phi_u(\gamma_u(t))|\mathbf{G}(t)]$ , where  $V \geq 0$  is the policy control parameter already introduced above, we have

$$\begin{aligned}
\Delta(\mathbf{G}(t)) - V \sum_{u \in \mathcal{U}} \mathbb{E}[\phi_u(\gamma_u(t))|\mathbf{G}(t)] &\leq \mathcal{K} - V \sum_{u \in \mathcal{U}} \mathbb{E}[\phi_u(\gamma_u(t))|\mathbf{G}(t)] + \mathbb{E}[(\mathbf{R}(t) - \boldsymbol{\mu}(t))^\top \mathbf{Q}(t)|\mathbf{G}(t)] \\
&\quad + \mathbb{E}[(\boldsymbol{\gamma}(t) - \mathbf{D}(t))^\top \boldsymbol{\Theta}(t)|\mathbf{G}(t)].
\end{aligned} \tag{29}$$

The DPP policy acquires information about  $\mathbf{G}(t)$  and  $\boldsymbol{\omega}(t)$  at every slot  $t$  and chooses  $a(t) \in A_{\boldsymbol{\omega}(t)}$  in order to minimize the right hand side of the above inequality. The non-constant part of this expression can be written as

$$\left[ \mathbf{R}^\top(t) \mathbf{Q}(t) - \mathbf{D}^\top(t) \boldsymbol{\Theta}(t) \right] - \left[ V \sum_{u \in \mathcal{U}} \phi_u(\gamma_u(t)) - \boldsymbol{\gamma}^\top(t) \boldsymbol{\Theta}(t) \right] - \boldsymbol{\mu}^\top(t) \mathbf{Q}(t). \quad (30)$$

The resulting control action  $a(t)$  is given by the minimization, at each chunk time  $t$ , of the expression in (30). Notice that the first term of (30) depends only on  $\mathbf{R}(t)$  and on  $m_u(t) \forall u \in \mathcal{U}$ , the second term of (30) depends only on  $\boldsymbol{\gamma}(t)$  and the third term of (30) depends only on  $\boldsymbol{\mu}(t)$ . Thus, the overall minimization decomposes into three separate sub-problems. The first sub-problem (related to the first term in (30)) consists of choosing the quality levels  $\{m_u(t)\}$  and the requested video-coding rates  $\{R_{hu}(t)\}$  for each user  $u$  and current chunk at time  $t$ . The second sub-problem (related to the second term in (30)) involves the greedy maximization of each user network utility function with respect to the auxiliary control variables  $\gamma_u(t)$ . The third sub-problem (related to the third term in (30)), consists of allocating the channel coding rates  $\mu_{hu}(t)$  for each helper  $h$  to its neighboring users  $u \in \mathcal{N}(h)$ .

Next, we show that the minimization of (30) yields the congestion control sub-policy at the users and the transmission scheduling sub-policy at the helpers given before.

1) *Derivation of the congestion control action:* The first term in (30) is given by

$$\sum_{u \in \mathcal{U}} \left\{ \sum_{h \in \mathcal{N}(u) \cap \mathcal{H}(f_u)} k Q_{hu}(t) R_{hu}(t) - \Theta_u(t) D_{f_u}(m_u(t), t) \right\}. \quad (31)$$

The minimization is achieved by minimizing separately each term inside the sum w.r.t.  $u$  with respect to  $m_u(t)$  and  $R_{hu}(t)$ . It is immediate to see that the solution consists of choosing the helper  $h_u^*(t)$  as in (10), the quality level as in (11) and requesting the whole chunk from helper  $h_u^*(t)$  at quality  $m_u(t)$ , i.e., letting  $R_{h_u^*(t)u}(t) = B_{f_u}(m_u(t), t)$ , as given in (12). The second term in (30), after a change of sign, is given by

$$\sum_{u \in \mathcal{U}} \{V \phi_u(\gamma_u(t)) - \gamma_u(t) \Theta_u(t)\}. \quad (32)$$

Again, this is maximized by maximizing separately each term, yielding (13).

2) *Derivation of the transmission scheduling action:* After a change of sign, the maximization of the third term in (30) yields precisely (14) where  $\mathcal{R}(t)$  is defined by the physical layer model of the network, and it is particularized to the cases of macro-diversity and unique association as discussed in Section III-A2.

It is worthwhile to notice here that our NUM approach can be applied to virtually any network with any physical layer (e.g., including non-universal frequency reuse, non-orthogonal intra-cel access, multiuser MIMO [40], cooperative network MIMO [4]). In fact, all what is needed is to characterize the network in terms of its achievable rate region  $\mathcal{R}(t)$ , when averaging with respect to the small-scale fading, and conditioning with respect to the slowly time-varying pathloss coefficients, that depend on the network topology and therefore on the users motion. Of course, for more complicated type of wireless physical layers, the description of  $\mathcal{R}(t)$  and therefore the solution of the corresponding MWSR problem (14) may be much more involved than in the cases treated here. For example, an extension of this approach to the case of multi-antenna helper nodes using multiuser MIMO is given in [41].

### C. Optimality

As outlined in Section II, VBR video yields time-varying quality and rate functions  $D_f(m, t)$  and  $B_f(m, t)$ , which depend on the individual video file. Furthermore, arbitrary user motion yields time variations of the path coefficients  $g_{hu}(t)$  at the same time-scale of the video streaming session. As a result, any stationarity or ergodicity assumption about the network state process  $\omega(t)$  is unlikely to hold in most practically relevant settings. Therefore, we consider the optimality of the DPP policy for an *arbitrary sample path* of the network state  $\omega(t)$ . Following in the footsteps of [24], [25], we compare the network utility achieved by our DPP policy with that achieved by an optimal oracle policy with  $T$ -slot lookahead, i.e., such knowledge of the future network states over an interval of length  $T$  slots. Time is split into frames of duration  $T$  slots and we consider  $F$  such frames. For an arbitrary sample path  $\omega(t)$ , we consider the static optimization problem over the  $j$ -th frame

$$\text{maximize} \quad \sum_{u \in \mathcal{U}} \phi_u \left( \frac{1}{T} \sum_{\tau=jT}^{(j+1)T-1} D_u(\tau) \right) \quad (33)$$

$$\text{subject to} \quad \frac{1}{T} \sum_{\tau=jT}^{(j+1)T-1} [kR_{hu}(\tau) - n\mu_{hu}(\tau)] \leq 0 \quad \forall (h, u) \in \mathcal{E} \quad (34)$$

$$a(t) \in A_{\omega(t)} \quad \forall t \in \{jT, \dots, (j+1)T-1\}, \quad (35)$$

and denote by  $\phi_j^{\text{opt}}$  the maximum of the network utility function for frame  $j$ , achieved over all policies which have future knowledge of the sample path  $\omega(t)$  over the  $j$ -th frame, subject to the constraint (34), which ensures that for every queue  $Q_{hu}$ , the total service provided over the frame is at least as large as the total arrivals in that frame. We have the following result:

*Theorem 1:* For the system defined in Section II, with state, scheduling policy and feasible action set given in Definitions 5, 2 and 3, respectively, the dynamic scheduling policy defined in Section III-A,

with control actions given in (9) – (16), achieves the per-sample path network utility

$$\sum_{u \in \mathcal{U}} \phi_u(\bar{D}_u) \geq \lim_{F \rightarrow \infty} \frac{1}{F} \sum_{j=0}^{F-1} \phi_j^{\text{opt}} - O\left(\frac{1}{V}\right) \quad (36)$$

with bounded queue backlogs satisfying

$$\lim_{F \rightarrow \infty} \frac{1}{FT} \sum_{\tau=0}^{FT-1} \left( \sum_{(h,u) \in \mathcal{E}} Q_{hu}(\tau) + \sum_{u \in \mathcal{U}} \Theta_u(\tau) \right) \leq O(V) \quad (37)$$

where  $O(1/V)$  indicates a term that vanishes as  $1/V$  and  $O(V)$  indicates a term that grows linearly with  $V$ , as the policy control parameter  $V$  grows large.  $\square$

*Proof:* See Appendix B.  $\blacksquare$

An immediate corollary of Theorem 1 is:

*Corollary 1:* For the system defined in Section II, when the network state is stationary and ergodic, then

$$\sum_{u \in \mathcal{U}} \phi_u(\bar{D}_u) \geq \phi^{\text{opt}} - O\left(\frac{1}{V}\right), \quad (38)$$

where  $\phi^{\text{opt}}$  is the optimal value of the NUM problem (7) in the stationary ergodic case,<sup>6</sup> and

$$\sum_{(h,u) \in \mathcal{E}} \bar{Q}_{hu} + \sum_{u \in \mathcal{U}} \bar{\Theta}_u \leq O(V) \quad (39)$$

In particular, if the network state is i.i.d., the bounding term in (38) is explicitly given by  $O(1/V) = \frac{\mathcal{K}}{V}$ , and the bounding term in (39) is explicitly given by  $\frac{\mathcal{K} + V(\phi_{\max} - \phi_{\min})}{\epsilon}$ , where  $\phi_{\min} = \sum_{u \in \mathcal{U}} \phi_u(D_u^{\min})$ ,  $\phi_{\max} = \sum_{u \in \mathcal{U}} \phi_u(D_u^{\max})$ ,  $\epsilon > 0$  is the slack variable corresponding to the constraint (34), and the constant  $\mathcal{K}$  is defined in (27).  $\square$

*Proof:* See Appendix B.  $\blacksquare$

#### IV. PRE-BUFFERING, RE-BUFFERING AND SKIPPING CHUNKS

As described in Section II, the playback process consumes chunks at fixed playback rate  $1/T_{\text{gop}}$  (one chunk per time slot), while the number of *ordered* chunks per unit time entering the playback buffer is a random variable, due to the fact that the network state  $\omega(t)$  is a random process (or an arbitrary varying function of time) and the transmission resources are dynamically allocated by the scheduling policy.

<sup>6</sup>Notice that in the stationary and ergodic case the value  $\phi^{\text{opt}}$  is generally achieved by an instantaneous policy with perfect knowledge of the state statistics or, equivalently, by a policy with infinite look-ahead, since the state statistics can be learned arbitrarily well from any sample path with probability 1, because of ergodicity.

Chunks must be ordered sequentially in order to be useful for video playback. If chunks go through different queues in the network and are affected by different delays, it may happen that already received chunks with higher order number cannot be used for playback until the missing chunks with lower order number are also received.

As we have noticed already in Section I and in Remark 1, our NUM problem formulation in (7) does not take into account the possibility of stall events, i.e., chunks that are not delivered within their playback deadline. This simplification has the advantage of yielding the simple and decentralized scheduling policy of Section III-A. However, in order to make such policy useful in practice we have to force the system to work in the smooth streaming regime, i.e., in the regime where the stall events have small probability. This can be done by adaptively determining the pre-buffering time  $T_u$  for each user  $u$  on the basis of an estimate of the largest delay of queues  $\{Q_{hu}(t) : h \in \mathcal{N}(u)\}$ . In this section, we propose a simple method that allows to determine  $T_u$  based on local information available at each user  $u$ .

An example of the playback buffer dynamics is illustrated in Table I and Fig. 1. The table indicates the chunk numbers and their respective arrival times. The blue curve in Fig. 1 shows the time evolution of the number of ordered chunks available in the playback buffer. The green curve indicates the evolution with time of the number of chunks consumed by playback. The playback consumption starts after an initial pre-buffering delay  $T_u = d$ , as indicated in the figure. At any instant  $t$ , the chunk requested at  $t - d$  is expected to be available in the playback buffer. However, if the chunk is delivered with a delay greater than  $d$ , the two curves meet and a stall event occurs. In order to prevent stall events, each user  $u$  should choose its pre-buffering time  $T_u$  to be larger than the maximum delay of the serving queues  $\{Q_{hu} : h \in \mathcal{N}(u) \cap \mathcal{H}(f_u)\}$ . Unfortunately, such maximum delay is neither deterministic nor known a priori.

We propose a scheme where each user  $u$  estimates its local delays by monitoring its delivery times in a sliding window spanning a fixed number of time slots. In addition, users can also skip a chunk if, by doing so, a sufficiently large jump-up in the number of ordered chunks in the playback buffer is achieved. For instance, in Table I and Fig. 1, the chunk which comes 4<sup>th</sup> in the ordered sequence arrives at the end of time slot 11. However, chunks numbered 5, 6, 7 and 8 arrive before slot 11 but cannot be played since 4 is missing. More generally, if chunk 4 were to arrive with a delay such that the number of chunks which arrive before 4 but come later in the ordered sequence becomes large, then the user could either continue waiting for the missing chunk and incur a stall event, or skip chunk 4 from playback and take advantage of the many already received chunks.

Let  $t_k$  denote the time slot in which a user requests the  $k^{\text{th}}$  chunk and let  $A_k$  be the time slot in which

TABLE I: Arrival times of chunks

Chunk number	1	2	3	4	5	6	7	8	9	10	11	12	13
Arrival time	3	4	5	11	6	8	9	10	12	13	16	15	14

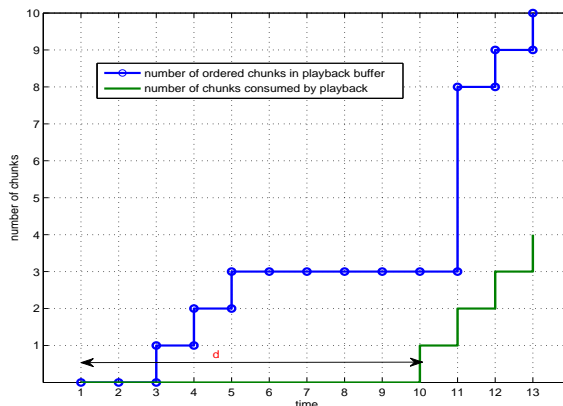


Fig. 1: Evolution of number of ordered and consumed chunks

the chunk arrives at the user playback buffer. The delay for chunk  $k$  is  $W_k = A_k - t_k$ . Without loss of generality, consider a user  $u$  starting its streaming session at time  $t = 1$ . In the proposed scheduling policy, user  $u$  requests one chunk per scheduling time, sequentially and possibly from different helpers, such that  $t_k = k$ . Since the chunks are downloaded from different helpers with different queue lengths and downlink channel capacities, they may be received out of order. For example, it may happen that  $A_k < A_j$  for some  $j < k$ . Hence, chunk  $k$  cannot be played until all chunks  $j$  for  $j < k$  are also received. We say that a chunk  $k$  becomes *playable* when all the chunks  $j \leq k$  are received. Let  $P_k$  denote the time when chunk  $k$  becomes *playable*. Then, we have:

$$P_k = \max\{A_1, A_2, \dots, A_k\}. \quad (40)$$

The proposed policy consists of two parts: skipping chunks from playback and buffering policy. We examine these two features separately in the following.

#### A. Skipping chunks from playback

Prior to slot  $t$ , the set of playable chunks is  $\{k : P_k \leq t - 1\}$  and

$$k_{t-1}^* = \max\{k : P_k \leq t - 1\} \quad (41)$$

is the highest-order chunk in the ordered sequence of playable chunks. At the end of slot  $t$ , user  $u$  considers the set  $\mathcal{C}_t$  of all chunks which have arrived before or during slot  $t$  and which come later than  $k_{t-1}^*$  in the ordered sequence of playback. The set  $\mathcal{C}_t$  is given by:

$$\mathcal{C}_t = \{k : k > k_{t-1}^*, A_k \leq t\}. \quad (42)$$

The next available chunk with order larger than  $k_{t-1}^*$  is given by:

$$k_t^- = \min\{k : k > k_{t-1}^*, A_k \leq t\}. \quad (43)$$

Let  $\mathcal{C}_t^* \subseteq \mathcal{C}_t$  be the set of chunks which become playable at the end of slot  $t$ , i.e.,

$$\mathcal{C}_t^* = \{k : A_k \leq t, P_k = t\}. \quad (44)$$

If  $k_t^-$  comes next to  $k_{t-1}^*$  in the playback order (i.e. if  $k_t^- = k_{t-1}^* + 1$ ), then  $\mathcal{C}_t^*$  is non-empty and all the chunks  $k \in \mathcal{C}_t^*$  can be added to the playback buffer. Further,  $k_t^*$  is recursively updated as:

$$k_t^* = k_{t-1}^* + |\mathcal{C}_t^*|. \quad (45)$$

Denoting the increment in the size of the playback buffer at the end of slot  $t$  by  $\Lambda_t$ , we have in this case that  $\Lambda_t = |\mathcal{C}_t^*|$ . On the other hand, if  $k_t^-$  is not the immediate successor of  $k_{t-1}^*$  in the playback order (i.e. if  $k_t^- > k_{t-1}^* + 1$ ), then there is no chunk in  $\mathcal{C}_t$  which becomes playable at the end of slot  $t$  and therefore  $\mathcal{C}_t^* = \emptyset$ . In this case, the algorithm compares  $|\mathcal{C}_t|$  with a threshold  $\rho$  in order to decide whether it should wait further for the missing chunk  $k_{t-1}^* + 1$  or skip it in order to increase the playback buffer anyway. The intuition behind such a decision is that it is worthwhile to skip a chunk if skipping such a chunk results in a large jump in the playback buffer size. The size of this possible jump can be exactly computed from  $\mathcal{C}_t$  as follows: assuming  $k_t^- = k_{t-1}^* + 2$ , if we skip chunk  $k_{t-1}^* + 1$ , then the increase in the playback buffer is given by the size of the set:

$$\{j \geq 2 : k_{t-1}^* + i \in \mathcal{C}_t \forall 2 \leq i \leq j\}.$$

We therefore propose the following policy: if  $|\mathcal{C}_t| \leq \rho$  (where  $\rho$  is a parameter  $> 0$ ), then wait for chunk  $k_{t-1}^* + 1$  and let  $k_t^* = k_{t-1}^*$ . Otherwise, if  $|\mathcal{C}_t| > \rho$ , the increase of the playback buffer is worthwhile and therefore it is useful to skip chunk  $k_{t-1}^* + 1$ . In this case, if  $k_t^- = k_{t-1}^* + 2$ , then  $k_t^*$  is updated as

$$k_t^* = k_{t-1}^* + \max\{j : k_{t-1}^* + i \in \mathcal{C}_t \forall 2 \leq i \leq j\} \quad (46)$$

and all the chunks numbered from  $k_{t-1}^* + 2$  to  $k_t^*$  are made playable at the end of slot  $t$  and added to the playback buffer. We therefore have  $\Lambda_t = |\{j > 2 : k_{t-1}^* + i \in \mathcal{C}_t \forall 2 \leq i \leq j\}|$  in this case. Instead, if  $k_t^- > k_{t-1}^* + 2$ , then the user skips chunk  $k_{t-1}^* + 1$  and starts waiting for chunk  $k_{t-1}^* + 2$ . Only a single

chunk is allowed to be skipped per slot because skipping multiple chunks might cause damage to the quality of experience of the user. Note that in this case,  $k_t^*$  is updated to  $k_{t-1}^* + 1$  even though the chunk  $k_{t-1}^* + 1$  is missing and is not playable. This is to ensure that when chunk  $k_{t-1}^* + 2$  is received, it is considered playable despite the fact that chunk  $k_{t-1}^* + 1$  is missing. Also note that there is no increment in the playback buffer (i.e.,  $\Lambda_t = 0$ ) in this case because there is no new chunk which becomes playable. Note that choosing  $\rho = \infty$  corresponds to the case when no chunk is skipped.

### B. Pre-buffering and re-buffering

The goal here is to determine the delay  $T_u$  after which user  $u$  should start playback, with respect to the time at which the first chunk is requested (beginning of the streaming session). Intuitively, choosing a large  $T_u$  makes the probability of stall events small. However, a too large  $T_u$  is very annoying for the user's quality of experience. From the chunk skipping strategy seen above, we know that  $\Lambda_t$  is the number of new chunks added to the playback buffer at the end of slot  $t$ . We define the size of the playback buffer  $\Psi_t$  as the number of playable chunks in the buffer not yet played. Without loss of generality, assume again that the streaming session starts at  $t = 1$ . Then,  $\Psi_t$  is recursively given by the updating equation:<sup>7</sup>

$$\Psi_t = \max\{\Psi_{t-1} - 1\{t > T_u\}, 0\} + \Lambda_t. \quad (47)$$

From the qualitative discussion on the evolution of the playback buffer at the beginning of Section IV, we notice that the longest period during which  $\Psi_t$  is not incremented (in the absence of chunk skipping decisions) is given by the maximum delay  $W_k$  to deliver chunks. In addition, we note that each user  $u$  needs to adaptively estimate  $W_k$  in order to choose  $T_u$ . In the proposed method, user  $u$  calculates for every chunk  $k$  the corresponding delay  $W_k = A_k - t_k$ . Notice that the delay of chunk  $k$ , can be calculated only at time  $A_k$ , i.e., when the chunk is actually delivered. At each time  $t = 1, 2, \dots$ , user  $u$  calculates the maximum observed delay  $E_t$  in a sliding window of size  $\Delta$ , (in all the numerical experiments in the sequel, we use  $\Delta = 10$ ) by letting:

$$E_t = \max\{W_k : t - \Delta + 1 \leq A_k \leq t\}. \quad (48)$$

Finally, user  $u$  starts its playback when  $\Psi_t$  crosses the level  $\xi E_t$ , i.e.,

$$T_u = \min\{t : \Psi_t \geq \xi E_t\}. \quad (49)$$

<sup>7</sup> $1\{\mathcal{A}\}$  denotes the indicator function of a condition or event  $\mathcal{A}$ .

If a stall event occurs at time  $t$ , i.e.,  $\Psi_t = 0$  for  $t > T_u$ , the algorithm enters a re-buffering phase in which the same algorithm presented above is employed again to determine the new instant  $t + T_u + 1$  at which playback is restarted. Notice that, with some abuse of notation, we have denoted the re-buffering delay again by  $T_u$  although this is re-estimated using the sliding window method at each new stall event. In fact, if a stall event occurs, it is likely that some change in the network state has occurred, such that the maximum delay must be re-estimated.

## V. NUMERICAL EXPERIMENTS, DISCUSSION AND CONCLUSIONS

In this section, we present two targeted numerical experiments illustrating the particular features of the proposed scheme. The first experiment considers the performance under a “macro-diversity” physical layer, for which the rate scheduling sub-problem takes on the form (15). We consider a large network with many stationary users and one mobile user moving across the network at constant speed. Users alternate between *idle* and *active* phases of video streaming. Each streaming session (when moving from idle to active state) is initialized using the pre-buffering scheme described in Section IV. This simulation demonstrates the dynamic and adaptive nature of the policy in response to variable bit-rate video coding and users joining or leaving the system at arbitrary times. Furthermore, the statistics relative to the streaming session of the mobile user shed light on the ability of the proposed algorithm to seamlessly discover new helper nodes as the user changes its position across the network. The second experiment considers a smaller network formed by four helpers and several users, in a situation of congestion for which most users are close to one helper. We consider the proposed scheme both under a “macro-diversity” and under “unique association” physical layer (where in the latter case, the rate scheduling problem takes on the form (17)) and compare its performance with a naive approach with max-SINR user-helper association, representative of today’s baseline technology.

As described in Section I, the helpers could be base stations connected to some video server through a wired backbone, or they could be dedicated wireless nodes with local caching capacity. For the sake of simplicity and replicability of our numerical results, here we assume that each helper has available the whole video library. Therefore, for any request  $f_u$  we have  $\mathcal{N}(u) \cap \mathcal{H}(f_u) = \mathcal{N}(u)$ . We use the utility function  $\phi_u(x) = \log(x)$  for all  $u \in \mathcal{U}$  (i.e., we use  $\alpha$ -fairness with  $\alpha = 1$  [36]). As described in Section II, a scheduling slot duration of 0.5s and a total available system bandwidth of  $W = 18$  MHz yield  $10^5$  LTE resource blocks per slot [2]. The total number of channel symbols  $n$  in a scheduling slot is  $10^5 \times 84$ . We assume that each user  $u$  has an edge to every helper  $h$  which satisfies  $nC_{hu}(t) > 1$  Mb (i.e., at least 2 Mb/s of peak rate).

The path loss coefficients  $g_{hu}(t)$  between helper  $h$  and user  $u$  are based on the WINNER II channel model [42]. In particular, we let

$$g_{hu}(t) = 10^{-\frac{\text{PL}(d_{hu}(t))}{10}},$$

where  $d_{hu}(t)$  is the distance from helper  $h$  to user  $u$  at time  $t$ , and where

$$\text{PL}(d) = A \log(d) + B + C \log(f_0/5) + \chi_{\text{dB}}. \quad (50)$$

In (50),  $d$  is expressed in meters, the carrier frequency  $f_0$  in GHz, and  $\chi_{\text{dB}}$  denotes a shadowing log-normal variable with variance  $\sigma_{\text{dB}}^2$ . The parameters  $A, B, C$  and  $\sigma_{\text{dB}}^2$  are scenario-dependent constants. Among the several models specified in WINNER II we chose the A1 model in [42], representative of a small-cell scenario. In this case,  $3 \leq d \leq 100$ , and the model parameters are given by  $A = 18.7$ ,  $B = 46.8$ ,  $C = 20$ ,  $\sigma_{\text{dB}}^2 = 9$  in line-of-sight (LOS) condition, or  $A = 36.8$ ,  $B = 43.8$ ,  $C = 20$ ,  $\sigma_{\text{dB}}^2 = 16$  in non-line-of-sight (NLOS) condition. For distances less than 3 m, we extended the model by setting  $\text{PL}(d) = \text{PL}(3)$ . Each link is in LOS or NLOS independently and at random, with probability  $p_l(d)$  and  $1 - p_l(d)$ , respectively, where

$$p_l(d) = \begin{cases} 1 & \text{if } d \leq 2.5\text{m} \\ 1 - 0.9(1 - (1.24 - 0.6 \log(d))^3)^{1/3} & \text{if else} \end{cases}$$

Every helper transmits at fixed power level  $P = 10^8$ .

Using Jensen's inequality in (2) to replacing the denominator of the SINR term with its average (this will be the average received inter-cell interference power), and the fact that the small-scale fading coefficients  $s_{hu}$  are  $\sim \mathcal{CN}(0, 1)$ , the peak achievable rates can be lower-bounded by the closed-form expression  $C_{hu}(t) = e^{1/\Gamma_{hu}(t)} \text{Ei}\left(1, \frac{1}{\Gamma_{hu}(t)}\right)$ , where  $\text{Ei}(1, x) = \int_x^\infty \frac{e^{-t}}{t} dt$  for  $x \geq 0$ , and  $\Gamma_{hu}(t) = \frac{P_h g_{hu}(t)}{1 + \sum_{h' \neq h} P_{h'} g_{h'u}(t)}$ . This formula, which provides a very accurate lower bound to (2) when the SINR denominator in (2) contains many independent terms, is an *achievable rate*<sup>8</sup> and is used in the numerical results of this section.

We assume that all the users request chunks successively from VBR-encoded video sequences. Each video file is a long sequence of chunks, each of duration 0.5 seconds and with a frame rate  $\eta = 30$  frames per second. We consider a specific video sequence formed by 800 chunks, constructed using 4 video clips from the database in [43], each of length 200 chunks. The chunks are encoded into different quality modes. Here, the quality index is measured using the *Structural SIMilarity* (SSIM) index defined in [44], Fig. s 2a and 2b show the size in kbits and the SSIM values as a function of the chunk index,

<sup>8</sup>A lower bound to an achievable rate is obviously achievable.

respectively, for the different quality modes. In our experiments, the chunks from 1 to 200 and 601 to 800 are encoded into 8 quality modes, while the chunks numbered from 201 to 600 are encoded in 4 quality modes. In both the experiments in the sequel, each user starts its streaming session of 1000 chunks from some arbitrary position in this reference video sequence and successively requests 1000 chunks by cycling through the sequence.

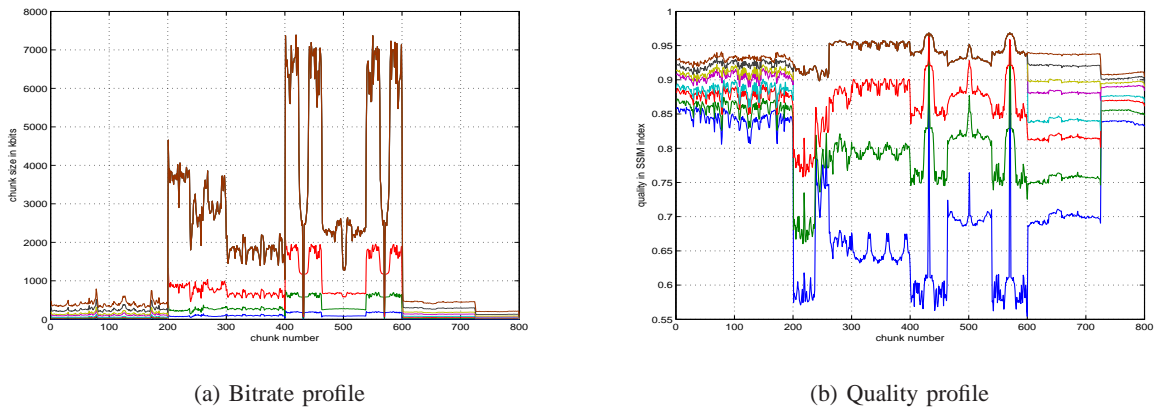


Fig. 2: Rate-quality profile of the test video sequence used in our simulations.

### A. Experiment 1

In the large network experiment, we consider a  $40\text{m} \times 40\text{m}$  square area divided into  $8 \times 8$  small square cells of side length  $5\text{m}$  as shown in Fig. 3. A helper is located at the center of each small square cell. The network includes 319 randomly placed stationary users and one mobile user whose trajectory is indicated by the green line. At  $t = 0$ , the mobile user starts a video streaming session of 1000 chunks. Simultaneously, it starts moving along the trajectory and stops after it requests the 1000<sup>th</sup> chunk. It doesn't request any more chunks after it stops moving. As the user moves through its trajectory, the new path loss coefficients  $g_{hu}(t)$  are calculated using the Winner II model said above, leading time-varying peak link rates  $C_{hu}(t)$ . The remaining 319 users in the system are stationary throughout the simulation period and alternate between *idle* and *active* phases of video streaming. At  $t = 0$ , all the stationary users are idle and each one of them independently starts a streaming session with probability  $p = 0.005$  at every slot. Thus, the time for which a user stays idle is geometrically distributed with mean  $\frac{1}{p} = 200$  slots. Once a user starts a streaming session, it stays *active* during 1000 video chunks. After finishing the requests, it goes back into the *idle* state and may start a new session after an independent and random

geometrically distributed idle time. We simulate the proposed scheme under the macro-diversity physical layer for 3000 slots for fixed values of the key parameters  $V$ ,  $\xi$  and  $\rho$  set to  $10^{13}$ , 25 and 50 respectively. These values have been chosen after extensive simulation and yields a good behavior of the scheduling policy. In general, the policy parameters have to be tuned to the specific network environment.

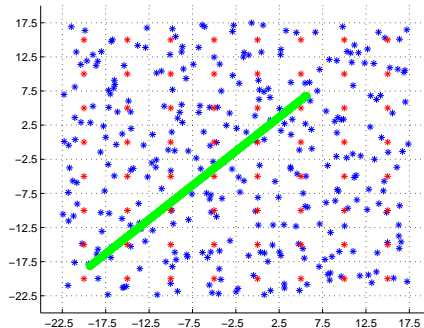


Fig. 3: Topology (the green line indicates the trajectory of the mobile user in Experiment 1).

We show the results in terms of the empirical CDF (over the user population) of the following metrics: 1) The percentage of skipped chunks spanning multiple streaming sessions of each user (Fig. 4d); 2) The quality (SSIM) averaged over the delivered chunks spanning multiple streaming sessions of each user (Fig. 4a); 3) The initial pre-buffering time (in number of slots) is calculated for each streaming session (Fig. 4b); 4) The percentage of time spent in *re-buffering* mode is calculated with respect to the total playback time spanning multiple streaming sessions of each user (Fig. 4c).

Focusing on the mobile user, we observe that the percentage of skipped chunks is 16% and the pre-buffering time is 180 time slots (i.e., 1min). Fig. 4e shows the evolution of the playback buffer  $\Phi_t$  over time. We notice that there is only one interruption (stall event) in the entire streaming session. The quality (SSIM) averaged over the delivered chunks is observed to be a high value of 0.87 (the maximum being 1.0). The helpers are numbered from 1 to 64, left to right and bottom to top, in Fig. 3. In Fig. 4f, we plot the helper index providing chunk  $k = 1, \dots, 1000$  vs. the chunk index. We can observe that as the user moves slowly along the path, the policy “discovers” adaptively the current neighboring helpers and downloads chunks from them in a seamless fashion. Overall, these results demonstrate the dynamic and adaptive nature of the proposed policy in response to user mobility, variable bit-rate video coding, and users joining or leaving the system at arbitrary times.

## B. Experiment 2

In this experiment, we focus on a smaller network with 4 helpers and 20 stationary users as indicated in Fig. 5a. The dimensions used for the topology are the same as in Fig. 3 where each of the 4 helpers is located at the centre of a  $5\text{m} \times 5\text{m}$  square cell and the overall area of the system is  $10\text{m} \times 10\text{m}$ . We consider a situation where the 20 users in the system are located close to the same helper, as indicated in Fig. 5a. We choose this non-uniform user distribution in order to investigate the load balancing property of the proposed policy in contrast to a naive scheme that allocates users to helpers based on maximum signal strength (or, equivalently, based on maximum SINR). In this experiment, all the 20 users start their streaming session simultaneously at  $t = 0$ , and stop after 1000 requested chunks. A baseline scheme, representative of current WLAN technology, performs client-based user-helper association, i.e., every user  $u$  chooses helper  $h_u^*(t) = \operatorname{argmax} \{C_{hu}(t) : h \in \mathcal{N}(u)\}$ . Then, the streaming process takes place accordingly by adapting the requested video quality according to DASH [27], [37]. We have emulated this situation by applying the same video quality level decisions as in (11), with user-helper association as given above.

We provide results for the proposed schemes with both “macro-diversity” and “unique association”. In order to simulate the unique association scheme, we solve the LP relaxation of (17) in every slot using the standard linear programming solver of MATLAB. In practice, this can be implemented by a centralized network controller. The results are shown in the form of empirical CDF (over the user population) of: 1) SSIM averaged over the chunks (Fig. 5b); 2) fraction of slots spent in buffering mode (including pre-buffering and re-buffering periods) (Fig. 5c); We notice that the proposed policy, both under macro-diversity and unique association, improves over the baseline scheme in terms of the video quality metric and the fraction of slots spent in buffering mode. This is because the baseline scheme a priori fixes the association of a user to the helper with best peak link rate, while the proposed schemes yield better load balancing by allowing each user to dynamically select the best helper in its neighborhood based on the congestion control decision (10), which takes into account the length of all queues “pointing” at the user itself. In addition, we notice that though the macro-diversity and the unique association schemes differ significantly in terms of implementation, the difference in terms of performance is small. This shows that 1) even in such a small cell scenario, macro-diversity does not provide a large gain over unique association;<sup>9</sup> 2) the major source of gain of the proposed 2) scheme over the base line scheme is due to

<sup>9</sup>Notice that in a macro-cell scenario, where most users are in good SINR conditions to at most one base station, macro-diversity would yield an even smaller performance gain over unique association.

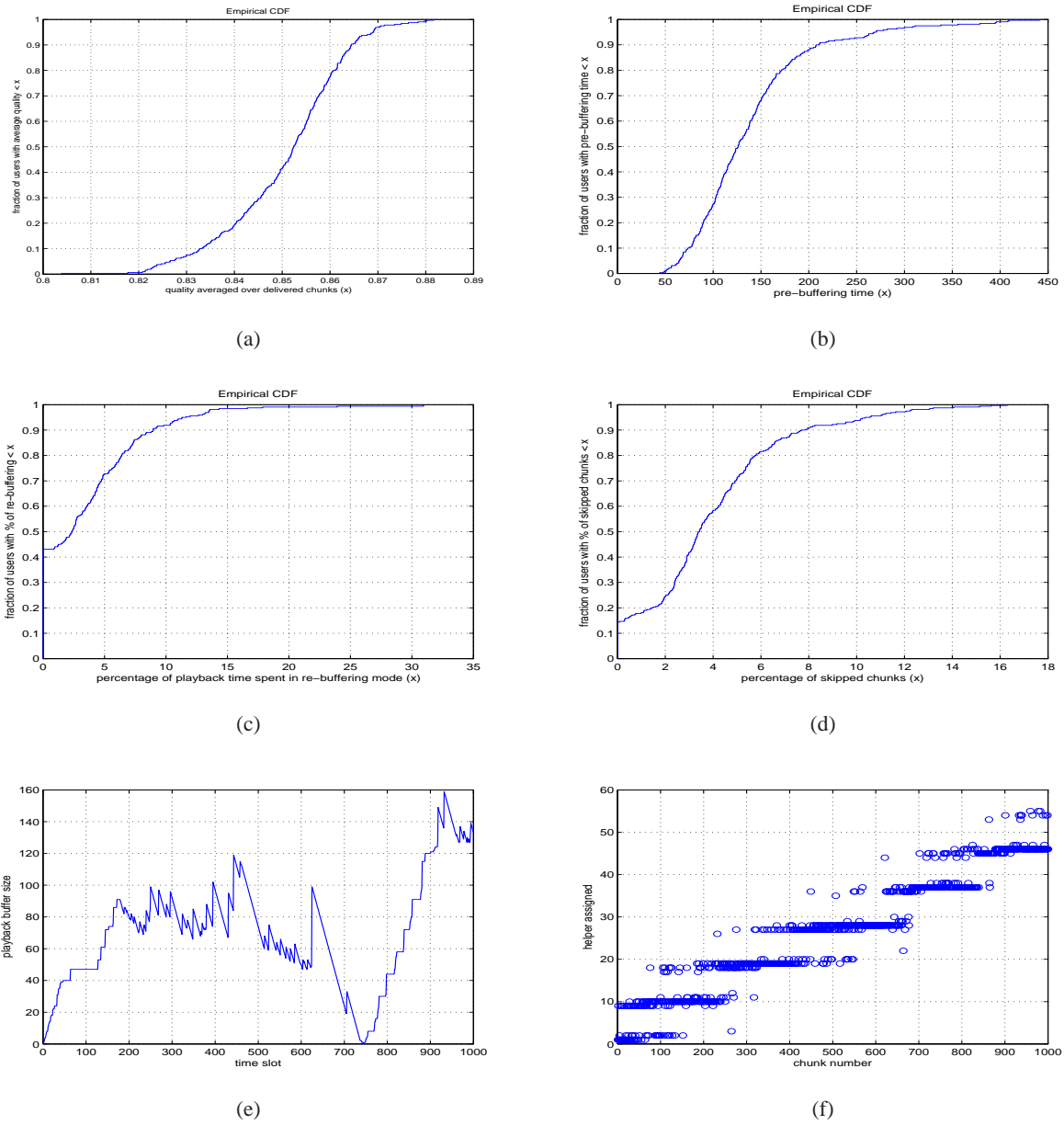


Fig. 4: CDFs of different performance metrics for Experiment 1.

its seamless load balancing property; 3) the main advantage of a macro-diversity physical layer over a physical layer where unique association is enforced consists of the simplicity of the decentralized nature of rate scheduling subproblem (15) over the centralized maximum weighted matching solution (17).

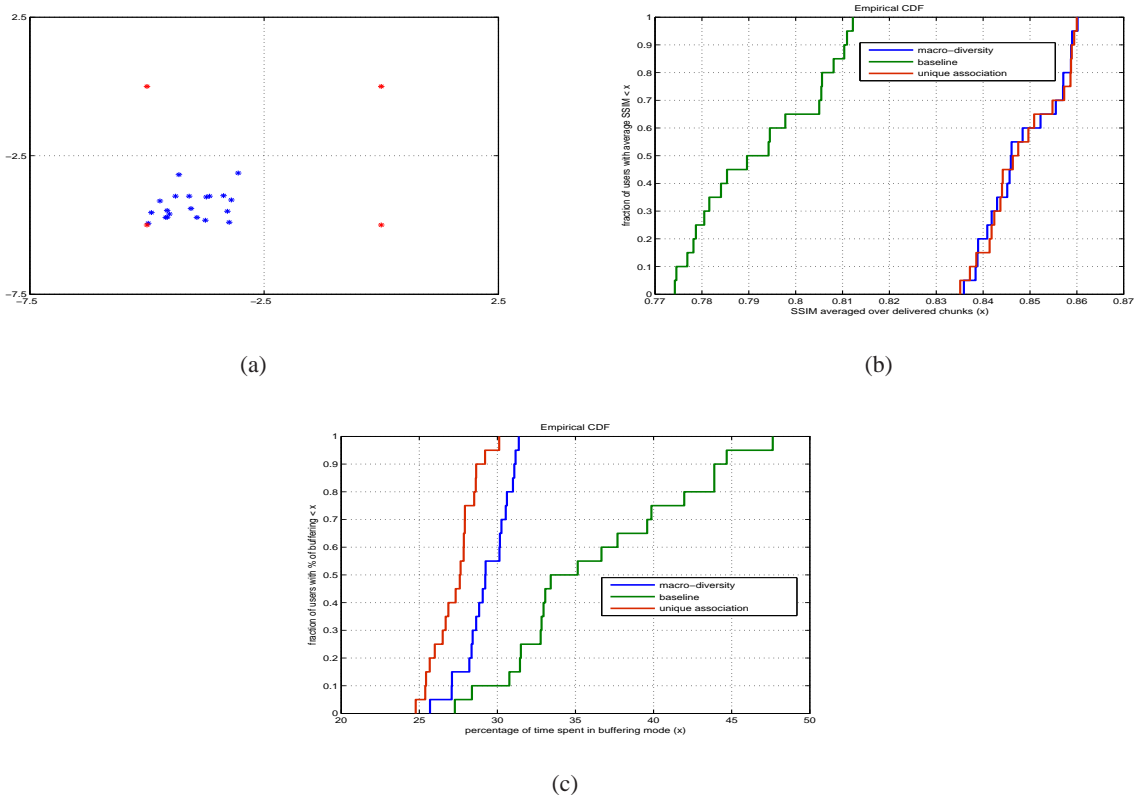


Fig. 5: Topology and CDFs of different performance metrics for Experiment 2.

## ACKNOWLEDGEMENT

This work is supported by the Intel/Cisco VAWN (video aware wireless networks) program. The authors would like to thank Hilmi Enes Egilmez and Prof. Antonio Ortega for providing a scalable encoded variable bitrate video sequence for the experiments and also for several useful discussions.

## APPENDIX A

### PROOF OF LEMMA 1

Let  $\phi_1^{\text{opt}}$  and  $\phi_2^{\text{opt}}$  be the optimal solutions of problems (7) and (18) – (22), respectively. Formally,  $\phi_1^{\text{opt}}$  is the supremum objective function value over all algorithms that satisfy the constraints of problem (7). The value  $\phi_2^{\text{opt}}$  is defined similarly. Now, fix  $\epsilon > 0$  and let  $a^*(t)$  be a policy that satisfies all constraints of the transformed problem (18) – (22) and achieves a utility not smaller than  $\phi_2^{\text{opt}} - \epsilon$ . We have

$$\phi_2^{\text{opt}} - \epsilon \leq \sum_{u \in \mathcal{U}} \overline{\phi_u(\gamma_u^*)} \stackrel{(a)}{\leq} \sum_{u \in \mathcal{U}} \phi_u(\overline{\gamma_u^*}) \stackrel{(b)}{\leq} \sum_{u \in \mathcal{U}} \phi_u(\overline{D_u^*}) \stackrel{(c)}{\leq} \phi_{\text{opt}}^1, \quad (51)$$

where (a) follows from Jensen's inequality applied to the concave function  $\phi_u(\cdot)$ , (b) follows by noticing that the policy  $a^*(t)$  satisfies the constraint (20) and  $\phi_u(\cdot)$  is non-decreasing, and (c) follows from the fact that since  $a^*(t)$  is feasible for problem (18) – (22), then it also satisfies the constraints of problem (7) and therefore it is feasible for the latter. As this holds for all  $\epsilon > 0$ , we conclude that  $\phi_2^{\text{opt}} \leq \phi_1^{\text{opt}}$ .

Now, let  $a'(t)$  be a policy for the original problem (7), achieving a utility not smaller than  $\phi_1^{\text{opt}} - \epsilon$ . Since  $a'(t)$  is feasible for (7), it also satisfies the constraints (19), (22) of the transformed problem. Further, we choose  $\gamma'(t) = \overline{\mathbf{D}}$  for all time  $t$ . Such choice of  $\gamma'(t)$  together with the policy  $a'(t)$  forms a feasible policy for problem (18) – (22). Therefore:

$$\phi_1^{\text{opt}} - \epsilon \leq \sum_{u \in \mathcal{U}} \phi_u(\overline{D}_u) = \sum_{u \in \mathcal{U}} \overline{\phi_u(\gamma'_u)} \leq \phi_2^{\text{opt}}. \quad (52)$$

As this holds for all  $\epsilon > 0$ , we conclude that  $\phi_1^{\text{opt}} \leq \phi_2^{\text{opt}}$ . Thus, (51) and (52) imply that  $\phi_1^{\text{opt}} = \phi_2^{\text{opt}}$  and, by comparing the constraint, it is immediate to conclude that an optimal policy for the transformed problem can be directly turned into an optimal policy for the original problem.

## APPENDIX B

### PROOF OF THEOREM 1 AND OF COROLLARY 1

As in Section III-B, we consider the following problem, equivalent to (33) – (35), which involves a sum of time-averages instead of functions of time averages and introduces the auxiliary variables  $\gamma_u(t)$ :

$$\text{maximize} \quad \frac{1}{T} \sum_{\tau=jT}^{(j+1)T-1} \sum_{u \in \mathcal{U}} \phi_u(\gamma_u(\tau)) \quad (53)$$

$$\text{subject to} \quad \frac{1}{T} \sum_{\tau=jT}^{(j+1)T-1} [kR_{hu}(\tau) - n\mu_{hu}(\tau)] \leq 0 \quad \forall (h, u) \in \mathcal{E} \quad (54)$$

$$\frac{1}{T} \sum_{\tau=jT}^{(j+1)T-1} [\gamma_u(\tau) - D_u(\tau)] \leq 0 \quad \forall u \in \mathcal{U} \quad (55)$$

$$D_u^{\min} \leq \gamma_u(t) \leq D_u^{\max} \quad \forall u \in \mathcal{U}, \quad \forall t \in \{jT, \dots, (j+1)T - 1\} \quad (56)$$

$$a(t) \in A_{\omega(t)} \quad \forall t \in \{jT, \dots, (j+1)T - 1\}. \quad (57)$$

The update equations for the transmission queues  $Q_{hu} \quad \forall (h, u) \in \mathcal{E}$  and the virtual queues  $\Theta_u \quad \forall u \in \mathcal{U}$  are given in (4) and in (9), respectively. Let  $\mathbf{G}(t) = [\mathbf{Q}^\top(t), \boldsymbol{\Theta}^\top(t)]^\top$  be the combined queue backlogs column vector, and define the quadratic Lyapunov function  $L(\mathbf{G}(t)) = \frac{1}{2} \mathbf{G}^\top(t) \mathbf{G}(t)$ . Fix a particular slot  $\tau$  in the  $j$ -th frame. We first consider the one-slot drift of  $L(\mathbf{G}(\tau))$ . From (26), we know that

$$L(\mathbf{G}(\tau + 1)) - L(\mathbf{G}(\tau)) \leq \mathcal{K} + (\mathbf{R}(t) - \boldsymbol{\mu}(\tau))^\top \mathbf{Q}(\tau) + (\gamma(\tau) - \mathbf{D}(t))^\top \boldsymbol{\Theta}(\tau) \quad (58)$$

where  $\mathcal{K}$  is a uniform bound on the term  $\frac{1}{2} [\boldsymbol{\mu}^\top(t)\boldsymbol{\mu}(t) + \mathbf{R}^\top(t)\mathbf{R}(t)] + \frac{1}{2} (\boldsymbol{\gamma}(t) - \mathbf{D}(t))^\top (\boldsymbol{\gamma}(t) - \mathbf{D}(t))$ , that exists under the realistic assumption that the source coding rates, the channel coding rates and the video quality measures are upper bounded by some constants, independent of  $t$ . We choose  $\mathcal{K}$  such that

$$\mathcal{K} > 2\boldsymbol{\kappa}^\top \boldsymbol{\kappa} \quad (59)$$

where  $\boldsymbol{\kappa}$  is a vector whose components are all equal to the same number  $\kappa$  and this number is a uniform upper bound on the maximum possible magnitude of drift in any of the queues (both actual and virtual) in one slot. With the additional penalty term  $-V \sum_{u \in \mathcal{U}} \phi_u(\gamma_u(\tau))$  added on both sides of (58), we have the following DPP inequality:

$$\begin{aligned} L(\mathbf{G}(\tau + 1)) - L(\mathbf{G}(\tau)) - V \sum_{u \in \mathcal{U}} \phi_u(\gamma_u(\tau)) &\leq \mathcal{K} + (\mathbf{R}(t) - \boldsymbol{\mu}(\tau))^\top \mathbf{Q}(\tau) + (\boldsymbol{\gamma}(\tau) - \mathbf{D}(t))^\top \boldsymbol{\Theta}(\tau) \\ &\quad - V \sum_{u \in \mathcal{U}} \phi_u(\gamma_u(\tau)) \end{aligned} \quad (60)$$

Let  $\{a(\tau)\}_{\tau=jT}^{(j+1)T-1}$  denote the DPP policy which minimizes the right hand side of the *drift plus penalty* inequality (60). Since it minimizes the expression on the RHS of (60), any other policy  $\{a^*(\tau)\}_{\tau=jT}^{(j+1)T-1}$  comprising of the decisions  $\{m_u^*(\tau)\}_{\tau=jT}^{(j+1)T-1}$ ,  $\{\mathbf{R}^*(\tau)\}_{\tau=jT}^{(j+1)T-1}$ ,  $\{\boldsymbol{\mu}^*(\tau)\}_{\tau=jT}^{(j+1)T-1}$  and  $\{\boldsymbol{\gamma}^*(\tau)\}_{\tau=jT}^{(j+1)T-1}$  would give a larger value of the expression. We therefore have

$$\begin{aligned} L(\mathbf{G}(\tau + 1)) - L(\mathbf{G}(\tau)) - V \sum_{u \in \mathcal{U}} \phi_u(\gamma_u(\tau)) &\leq \mathcal{K} + (\mathbf{R}^*(\tau) - \boldsymbol{\mu}^*(\tau))^\top \mathbf{Q}(\tau) + (\boldsymbol{\gamma}^*(\tau) - \mathbf{D}^*(\tau))^\top \boldsymbol{\Theta}(\tau) \\ &\quad - V \sum_{u \in \mathcal{U}} \phi_u(\gamma_u^*(\tau)). \end{aligned} \quad (61)$$

Further, we note that the maximum change in the queue length vectors  $Q_{hu}(\tau)$  and  $\Theta_u(\tau)$  from one slot to the next is bounded by  $\kappa$ . Thus, we have for all  $\tau \in \{jT, \dots, (j+1)T - 1\}$

$$|Q_{hu}(\tau) - Q_{hu}(jT)| \leq (\tau - jT)\kappa \quad \forall (h, u) \in \mathcal{E} \quad (62)$$

$$|\Theta_u(\tau) - \Theta_u(jT)| \leq (\tau - jT)\kappa \quad \forall u \in \mathcal{U} \quad (63)$$

Substituting the above inequalities in (61), we have

$$\begin{aligned} L(\mathbf{G}(\tau + 1)) - L(\mathbf{G}(\tau)) - V \sum_{u \in \mathcal{U}} \phi_u(\gamma_u(\tau)) &\leq \mathcal{K} + (\mathbf{R}^*(\tau) - \boldsymbol{\mu}^*(\tau))^\top (\mathbf{Q}(jT) + (\tau - jT)\boldsymbol{\kappa}) \\ &\quad + (\boldsymbol{\gamma}^*(\tau) - \mathbf{D}^*(\tau))^\top (\boldsymbol{\Theta}(jT) + (\tau - jT)\boldsymbol{\kappa}) \\ &\quad - V \sum_{u \in \mathcal{U}} \phi_u(\gamma_u^*(\tau)). \end{aligned} \quad (64)$$

Then, summing (64) over  $\tau \in \{jT, \dots, (j+1)T-1\}$ , we obtain the  $T$ -slot Lyapunov drift over the  $j$ -th frame:

$$\begin{aligned}
& L(\mathbf{G}((j+1)T)) - L(\mathbf{G}(jT)) - V \sum_{\tau=jT}^{jT+T-1} \sum_{u \in \mathcal{U}} \phi_u(\gamma_u(\tau)) \\
& \leq \mathcal{K}T + \left( \sum_{\tau=jT}^{jT+T-1} (\mathbf{R}^*(\tau) - \boldsymbol{\mu}^*(\tau)) \right)^\top \mathbf{Q}(jT) + \left( \sum_{\tau=jT}^{jT+T-1} (\mathbf{R}^*(\tau) - \boldsymbol{\mu}^*(\tau)) (\tau - jT) \right)^\top \boldsymbol{\kappa} \\
& \quad + \left( \sum_{\tau=jT}^{jT+T-1} (\boldsymbol{\gamma}^*(\tau) - \mathbf{D}^*(\tau)) \right)^\top \boldsymbol{\Theta}(jT) + \left( \sum_{\tau=jT}^{jT+T-1} (\boldsymbol{\gamma}^*(\tau) - \mathbf{D}^*(\tau)) (\tau - jT) \right)^\top \boldsymbol{\kappa} \\
& \quad - V \sum_{\tau=jT}^{jT+T-1} \sum_{u \in \mathcal{U}} \phi_u(\gamma_u^*(\tau)) \tag{65}
\end{aligned}$$

Using the inequalities  $\mathbf{R}^*(\tau) - \boldsymbol{\mu}^*(\tau) \leq 2\boldsymbol{\kappa}$ ,  $\boldsymbol{\gamma}^*(\tau) - \mathbf{D}^*(\tau) \leq 2\boldsymbol{\kappa}$  in (65), we have

$$\begin{aligned}
& L(\mathbf{G}((j+1)T)) - L(\mathbf{G}(jT)) - V \sum_{\tau=jT}^{jT+T-1} \sum_{u \in \mathcal{U}} \phi_u(\gamma_u(\tau)) \\
& \leq \mathcal{K}T + \left( \sum_{\tau=jT}^{jT+T-1} (\mathbf{R}^*(\tau) - \boldsymbol{\mu}^*(\tau)) \right)^\top \mathbf{Q}(jT) + 2 \left( \sum_{\tau=jT}^{jT+T-1} (\tau - jT) \right) \boldsymbol{\kappa}^\top \boldsymbol{\kappa} \\
& \quad + \left( \sum_{\tau=jT}^{jT+T-1} (\boldsymbol{\gamma}^*(\tau) - \mathbf{D}^*(\tau)) \right)^\top \boldsymbol{\Theta}(jT) + 2 \left( \sum_{\tau=jT}^{jT+T-1} (\tau - jT) \right) \boldsymbol{\kappa}^\top \boldsymbol{\kappa} \\
& \quad - V \sum_{\tau=jT}^{jT+T-1} \sum_{u \in \mathcal{U}} \phi_u(\gamma_u^*(\tau)) \tag{66}
\end{aligned}$$

Using  $\boldsymbol{\kappa}^\top \boldsymbol{\kappa} \leq \frac{\mathcal{K}}{2}$ ,  $\sum_{\tau=jT}^{jT+T-1} (\tau - jT) = \frac{T(T-1)}{2}$ , we get

$$\begin{aligned}
& L(\mathbf{G}((j+1)T)) - L(\mathbf{G}(jT)) - V \sum_{\tau=jT}^{jT+T-1} \sum_{u \in \mathcal{U}} \phi_u(\gamma_u(\tau)) \\
& \leq \mathcal{K}T + \mathcal{K}T(T-1) + \left( \sum_{\tau=jT}^{jT+T-1} (\mathbf{R}^*(\tau) - \boldsymbol{\mu}^*(\tau)) \right)^\top \mathbf{Q}(jT) \\
& \quad + \left( \sum_{\tau=jT}^{jT+T-1} (\boldsymbol{\gamma}^*(\tau) - \mathbf{D}^*(\tau)) \right)^\top \boldsymbol{\Theta}(jT) - V \sum_{\tau=jT}^{jT+T-1} \sum_{u \in \mathcal{U}} \phi_u(\gamma_u^*(\tau)) \tag{67}
\end{aligned}$$

We now consider the policy  $\{a^*(\tau)\}_{\tau=jT}^{(j+1)T-1}$  satisfying the following constraints:<sup>10</sup>

$$\frac{1}{T} \sum_{\tau=jT}^{(j+1)T-1} [kR_{hu}^*(\tau) - n\mu_{hu}^*(\tau)] < -\epsilon \quad \forall (h, u) \in \mathcal{E} \quad (68)$$

$$\frac{1}{T} \sum_{\tau=jT}^{(j+1)T-1} [\gamma_u^*(\tau) - D_u^*(\tau)] < -\epsilon \quad \forall u \in \mathcal{U} \quad (69)$$

where  $\epsilon > 0$  is arbitrary. We plug in the inequalities (68), (69) in (67) and obtain

$$\begin{aligned} L(\mathbf{G}((j+1)T)) - L(\mathbf{G}(jT)) - V \sum_{\tau=jT}^{jT+T-1} \sum_{u \in \mathcal{U}} \phi_u(\gamma_u(\tau)) \\ < \mathcal{K}T^2 - \epsilon T \sum_{(h,u) \in \mathcal{E}} Q_{hu}(jT) - \epsilon T \sum_{u \in \mathcal{U}} \Theta_u(jT) - V \sum_{\tau=jT}^{jT+T-1} \sum_{u \in \mathcal{U}} \phi_u(\gamma_u^*(\tau)) \end{aligned} \quad (70)$$

Also, considering the fact that for any vector  $\gamma = (\gamma_1, \dots, \gamma_{|\mathcal{U}|})$  we have

$$\sum_{u \in \mathcal{U}} \phi_u(D_u^{\min}) = \phi_{\min} \leq \sum_{u \in \mathcal{U}} \phi_u(\gamma_u) \leq \phi_{\max} = \sum_{u \in \mathcal{U}} \phi_u(D_u^{\max}), \quad (71)$$

we can write:

$$L(\mathbf{G}((j+1)T)) - L(\mathbf{G}(jT)) < \mathcal{K}T^2 + VT(\phi_{\max} - \phi_{\min}) - \epsilon T \sum_{(h,u) \in \mathcal{E}} Q_{hu}(jT) - \epsilon T \sum_{u \in \mathcal{U}} \Theta_u(jT) \quad (72)$$

Once again using (62), (63), we have:

$$\begin{aligned} L(\mathbf{G}((j+1)T)) - L(\mathbf{G}(jT)) < \mathcal{K}T^2 + VT(\phi_{\max} - \phi_{\min}) - \epsilon \sum_{\tau=jT}^{jT+T-1} \sum_{(h,u) \in \mathcal{E}} Q_{hu}(\tau) \\ - \epsilon \sum_{\tau=jT}^{jT+T-1} \sum_{u \in \mathcal{U}} \Theta_u(\tau) + \frac{\epsilon \kappa (|\mathcal{E}| + |\mathcal{U}|) T (T-1)}{2} \end{aligned} \quad (73)$$

Summing the above over the frames  $j \in \{0, \dots, F-1\}$  yields

$$\begin{aligned} L(\mathbf{G}(FT)) - L(\mathbf{G}(0)) < \mathcal{K}T^2 F + VFT(\phi_{\max} - \phi_{\min}) - \epsilon \sum_{\tau=0}^{FT-1} \sum_{(h,u) \in \mathcal{E}} Q_{hu}(\tau) \\ - \epsilon \sum_{\tau=0}^{FT-1} \sum_{u \in \mathcal{U}} \Theta_u(\tau) + \frac{\epsilon \kappa (|\mathcal{E}| + |\mathcal{U}|) FT (T-1)}{2} \end{aligned} \quad (74)$$

<sup>10</sup>It is easy to see that such policy is guaranteed to exist provided that we allow, without loss of generality, for a virtual video layer of zero quality and zero rate, and in the assumption that, at any time  $t$ , each user  $u$  has at least one link  $(h, u) \in \mathcal{E}$  with  $h \in \mathcal{N}(u) \cap \mathcal{H}(f_u)$  with peak rate  $C_{hu}(t)$  lower bounded by some strictly positive number  $C_{\min}$ . This prevents the case where a user gets zero rate for a whole frame of length  $T$ . This assumption is not restrictive in practice since a user experiencing unacceptably poor link quality to all the helpers for a long time interval would be disconnected from the network and its streaming session halted.

Rearranging and neglecting appropriate terms, we get

$$\begin{aligned} \frac{1}{FT} \sum_{\tau=0}^{FT-1} \sum_{(h,u) \in \mathcal{E}} Q_{hu}(\tau) + \frac{1}{FT} \sum_{\tau=0}^{FT-1} \sum_{u \in \mathcal{U}} \Theta_u(\tau) &< \frac{\mathcal{K}T}{\epsilon} + \frac{V(\phi_{\max} - \phi_{\min})}{\epsilon} + \frac{L(\mathbf{G}(0))}{\epsilon FT} \\ &+ \frac{\kappa(|\mathcal{E}| + |\mathcal{U}|)(T-1)}{2} \end{aligned} \quad (75)$$

Taking limits as  $F \rightarrow \infty$

$$\boxed{\lim_{F \rightarrow \infty} \frac{1}{FT} \sum_{\tau=0}^{FT-1} \left( \sum_{(h,u) \in \mathcal{E}} Q_{hu}(\tau) + \sum_{u \in \mathcal{U}} \Theta_u(\tau) \right) < \frac{\mathcal{K}T}{\epsilon} + \frac{V(\phi_{\max} - \phi_{\min})}{\epsilon} + \frac{\kappa(|\mathcal{E}| + |\mathcal{U}|)(T-1)}{2}} \quad (76)$$

such that (37) is proved.

We now consider the policy  $\{a^*(\tau)\}_{\tau=jT}^{(j+1)T-1}$  which achieves the optimal solution  $\phi_j^{\text{opt}}$  to the problem (53) – (57). Using (54) and (55) in (67), we have

$$L(\mathbf{G}((j+1)T)) - L(\mathbf{G}(jT)) - V \sum_{\tau=jT}^{jT+T-1} \sum_{u \in \mathcal{U}} \phi_u(\gamma_u(\tau)) \leq \mathcal{K}T + \mathcal{K}T(T-1) - VT\phi_j^{\text{opt}} \quad (77)$$

Summing this over  $j \in \{0, \dots, F-1\}$ , yields

$$L(\mathbf{G}((FT)) - L(\mathbf{G}(0)) - V \sum_{\tau=0}^{FT-1} \sum_{u \in \mathcal{U}} \phi_u(\gamma_u(\tau)) \leq \mathcal{K}T^2 F - VT \sum_{j=0}^{F-1} \phi_j^{\text{opt}}. \quad (78)$$

Dividing both sides by  $VFT$  and using the fact that  $L(\mathbf{G}((FT)) > 0$ , we get

$$\frac{1}{FT} \sum_{\tau=0}^{FT-1} \sum_{u \in \mathcal{U}} \phi_u(\gamma_u(\tau)) \geq \frac{1}{F} \sum_{j=0}^{F-1} \phi_j^{\text{opt}} - \frac{\mathcal{K}T}{V} - \frac{L(\mathbf{G}(0))}{VTF}. \quad (79)$$

At this point, using Jensen's inequality, the fact that  $\phi_u(\cdot)$  is continuous and non-decreasing for all  $u \in \mathcal{U}$ , and the fact that the strong stability of the queues (76) implies that  $\lim_{F \rightarrow \infty} \frac{1}{FT} \sum_{\tau=0}^{FT-1} \Theta_u(\tau) < \infty \forall u \in \mathcal{U}$ , which in turns implies that  $\bar{\gamma}_u \leq \bar{D}_u \forall u \in \mathcal{U}$ , we arrive at

$$\boxed{\sum_{u \in \mathcal{U}} \phi_u(\bar{D}_u) \geq \lim_{F \rightarrow \infty} \frac{1}{F} \sum_{j=0}^{F-1} \phi_j^{\text{opt}} - \frac{\mathcal{K}T}{V}.} \quad (80)$$

such that (36) is proved.

Thus, the utility under the DPP policy is within  $O(1/V)$  of the time average of the  $\phi_j^{\text{opt}}$  utility values that can be achieved only if knowledge of the future states up to a look-ahead of blocks of  $T$  slots. If  $T$  is increased, then the value of  $\phi_j^{\text{opt}}$  for every frame  $j$  improves since we allow a larger look-ahead. However, from (80), we can see that if  $T$  is increased, then  $V$  can also be increased in order to maintain the same distance from optimality. This yields a corresponding  $O(V)$  increase in the queues backlog.

For the case where the network state  $\omega(t)$  is stationary and ergodic, the time average in the left hand side of (76) and in the right hand side of (80) become ensemble averages because of ergodicity. Thus, we obtain (38) and (39). Furthermore, if the network state is i.i.d., we can take  $T = 1$  in the above derivation, obtaining the bounds given in Corollary 1.

## REFERENCES

- [1] [Online]. Available: <http://www.cisco.com/en/US/solutions/collateral/ns341/ns525/ns537/ns705/ns827/white/paper/c11-520862.html>
- [2] S. Sesia, I. Toufik, and M. Baker, *LTE: the Long Term Evolution-From theory to practice*. Wiley, 2009.
- [3] T. L. Marzetta, “Noncooperative cellular wireless with unlimited numbers of base station antennas,” *IEEE Trans. on Wireless Communications*, vol. 9, no. 11, pp. 3590–3600, Nov. 2010.
- [4] H. Huh, G. Caire, H. Papadopoulos, and S. Ramprasad, “Achieving massive MIMO spectral efficiency with a not-so-large number of antennas,” *IEEE Trans. on Wireless Communications*, vol. 11, no. 9, pp. 3226–3239, 2012.
- [5] J. Hoydis, S. Ten Brink, and M. Debbah, “Massive MIMO: How many antennas do we need?” in *2011 49th Annual Allerton Conference on Communication, Control, and Computing (Allerton)*. IEEE, 2011, pp. 545–550.
- [6] V. Chandrasekhar, J. Andrews, and A. Gatherer, “Femtocell networks: a survey,” *Communications Magazine, IEEE*, vol. 46, no. 9, pp. 59–67, 2008.
- [7] J. Hoydis, M. Kobayashi, and M. Debbah, “Green small-cell networks,” *Vehicular Technology Magazine, IEEE*, vol. 6, no. 1, pp. 37–43, 2011.
- [8] C. wei Tan, “Optimal power control in rayleigh-fading heterogeneous networks,” in *INFOCOM, 2011 Proceedings IEEE*, April 2011, pp. 2552–2560.
- [9] M. Ji, G. Caire, and A. F. Molisch, “Optimal throughput-outage trade-off in wireless one-hop caching networks,” *arXiv preprint arXiv:1302.2168*, 2013.
- [10] —, “Wireless device-to-device caching networks: Basic principles and system performance,” *arXiv preprint arXiv:1305.5216*, 2013.
- [11] N. Golrezaei, A. F. Molisch, A. G. Dimakis, and G. Caire, “Femtocaching and device-to-device collaboration: A new architecture for wireless video distribution,” *Communications Magazine, IEEE*, vol. 51, no. 4, pp. 142–149, 2013.
- [12] K. Shanmugam, N. Golrezaei, A. G. Dimakis, A. F. Molisch, and G. Caire, “Femtocaching: Wireless video content delivery through distributed caching helpers,” *arXiv preprint arXiv:1109.4179*, 2011.
- [13] N. Golrezaei, K. Shanmugam, A. G. Dimakis, A. F. Molisch, and G. Caire, “Femtocaching: Wireless video content delivery through distributed caching helpers,” in *INFOCOM, 2012 Proceedings IEEE*. IEEE, 2012, pp. 1107–1115.
- [14] —, “Wireless video content delivery through coded distributed caching,” in *Communications (ICC), 2012 IEEE International Conference on*. IEEE, 2012, pp. 2467–2472.
- [15] M. A. Maddah-Ali and U. Niesen, “Fundamental limits of caching,” in *Information Theory Proceedings (ISIT), 2013 IEEE International Symposium on*. IEEE, 2013, pp. 1077–1081.
- [16] —, “Decentralized coded caching attains order-optimal memory-rate tradeoff,” *arXiv preprint arXiv:1301.5848*, 2013.
- [17] U. Niesen and M. A. Maddah-Ali, “Coded caching with nonuniform demands,” *arXiv preprint arXiv:1308.0178*, 2013.
- [18] R. Pedarsani, M. A. Maddah-Ali, and U. Niesen, “Online coded caching,” *arXiv preprint arXiv:1311.3646*, 2013.
- [19] M. Ji, A. M. Tulino, J. Llorca, and G. Caire, “Order optimal coded caching-aided multicast under zipf demand distributions,” *arXiv preprint arXiv:1402.4576*, 2014.

- [20] M. Ji, G. Caire, and A. F. Molisch, "Fundamental limits of distributed caching in d2d wireless networks," in *Information Theory Workshop (ITW), 2013 IEEE*. IEEE, 2013, pp. 1–5.
- [21] F. Kelly, "The mathematics of traffic in networks," *The Princeton Companion to Mathematics*, 2006.
- [22] Y. Yi and M. Chiang, "Stochastic network utility maximisation—a tribute to Kelly’s paper published in this journal a decade ago," *European Transactions on Telecommunications*, vol. 19, no. 4, pp. 421–442, 2008.
- [23] M. Chiang, S. Low, A. Calderbank, and J. Doyle, "Layering as optimization decomposition: A mathematical theory of network architectures," *Proceedings of the IEEE*, vol. 95, no. 1, pp. 255–312, 2007.
- [24] M. Neely, "Stochastic network optimization with application to communication and queueing systems," *Synthesis Lectures on Communication Networks*, vol. 3, no. 1, pp. 1–211, 2010.
- [25] —, "Universal scheduling for networks with arbitrary traffic, channels, and mobility," in *Decision and Control (CDC), 2010 49th IEEE Conference on*. IEEE, 2010, pp. 1822–1829.
- [26] A. Ortega, "Variable bit-rate video coding," *Compressed Video over Networks*, pp. 343–382, 2000.
- [27] Y. Sánchez, T. Schierl, C. Hellge, T. Wiegand, D. Hong, D. De Vleeschauwer, W. Van Leekwijck, and Y. Lelouedec, "iDASH: improved dynamic adaptive streaming over HTTP using scalable video coding," in *ACM Multimedia Systems Conference (MMSys)*, 2011, pp. 23–25.
- [28] A. Begen, T. Akgul, and M. Baugher, "Watching video over the web: Part 1: Streaming protocols," *Internet Computing, IEEE*, vol. 15, no. 2, pp. 54–63, 2011.
- [29] Z. Wang, A. Bovik, H. Sheikh, and E. Simoncelli, "Image quality assessment: From error visibility to structural similarity," *Image Processing, IEEE Transactions on*, vol. 13, no. 4, pp. 600–612, 2004.
- [30] T. Ho, M. Médard, R. Koetter, D. R. Karger, M. Effros, J. Shi, and B. Leong, "A random linear network coding approach to multicast," *Information Theory, IEEE Transactions on*, vol. 52, no. 10, pp. 4413–4430, 2006.
- [31] D. Tse and P. Viswanath, *Fundamentals of wireless communication*. Cambridge Univ Pr, 2005.
- [32] T. Richardson and R. L. Urbanke, *Modern coding theory*. Cambridge University Press, 2008.
- [33] E. Biglieri, J. Proakis, and S. Shamai, "Fading channels: Information-theoretic and communications aspects," *Information Theory, IEEE Transactions on*, vol. 44, no. 6, pp. 2619–2692, 1998.
- [34] E. H. Ong, J. Knecht, O. Alanen, Z. Chang, T. Huovinen, and T. Nihtila, "IEEE 802.11 ac: Enhancements for very high throughput WLANs," in *2011 IEEE 22nd International Symposium on Personal Indoor and Mobile Radio Communications (PIMRC)*. IEEE, 2011, pp. 849–853.
- [35] A. F. Molisch, *Wireless communications*. Wiley, 2010, vol. 15.
- [36] J. Mo and J. Walrand, "Fair end-to-end window-based congestion control," *IEEE/ACM Transactions on Networking (ToN)*, vol. 8, no. 5, pp. 556–567, 2000.
- [37] Y. Sanchez, T. Schierl, C. Hellge, T. Wiegand, D. Hong, D. De Vleeschauwer, W. Van Leekwijck, and Y. Lelouedec, "Improved caching for HTTP-based video on demand using scalable video coding," in *Consumer Communications and Networking Conference (CCNC), 2011 IEEE*. IEEE, 2011, pp. 595–599.
- [38] A. Schrijver, *Combinatorial optimization: polyhedra and efficiency*. Springer, 2003, vol. 24.
- [39] N. Bhushan, C. Lott, P. Black, R. Attar, Y.-C. Jou, M. Fan, D. Ghosh, and J. Au, "CDMA2000 1× EV-DO revision a: a physical layer and mac layer overview," *Communications Magazine, IEEE*, vol. 44, no. 2, pp. 37–49, 2006.
- [40] G. Caire, N. Jindal, M. Kobayashi, and N. Ravindran, "Multiuser mimo achievable rates with downlink training and channel state feedback," *Information Theory, IEEE Transactions on*, vol. 56, no. 6, pp. 2845–2866, 2010.

- [41] D. Bethanabhotla, G. Caire, and M. J. Neely, "Adaptive video streaming in mu-mimo networks," *arXiv preprint arXiv:1401.6476*, 2014.
- [42] P. Kyosti, J. Meinila, L. Hentila, X. Zhao, T. Jamsa, C. Schneider, M. Narandzic, M. Milojevic, A. Hong, J. Ylitalo *et al.*, "WINNER II channel models," *European Commission, Deliverable IST-WINNER D*, vol. 1, 2007.
- [43] <http://media.xiph.org/video/derf/>.
- [44] <https://ece.uwaterloo.ca/~z70wang/research/ssim/>.